



From the Department of Neurology

of University Würzburg

Director: Professor Jens Volkmann

Progressive alterations of pro- and antidegeneration markers in the nigrostriatal tract
of the AAV1/2-A53T- α synuclein rat model of Parkinson's disease

Doctoral thesis for a doctoral degree

at medical faculty of

Julius-Maximilians-University Würzburg,

submitted by

Jing Yin

From Changsha, China

Würzburg, July 2021

Speaker: apl. Prof. Dr. med. habil. Chi Wang Ip

Co-referee: Univ.-Prof. Dr. med. Süleyman Ergün

Dean: Univ.-Prof. Dr. Matthias Frosch

Date of the oral examination: 01.03.2022

The doctoral candidate is a medical doctor

1	Introduction.....	1
1.1	Parkinson’s disease (PD).....	1
1.2	Etiology of PD	1
1.2.1	Environmental factors	1
1.2.2	Genetic causes.....	2
1.2.2.1	SNCA	2
1.2.2.2	LRRK-2.....	3
1.2.2.3	Recessive genes	4
1.3	Animal models of PD	4
1.3.1	Neurotoxic models	4
1.3.1.1	6-hydroxydopamine (6-OHDA) model.....	4
1.3.1.2	MPTP model	5
1.3.1.3	Rotenone model	6
1.3.1.4	Herbicide (Paraquat) model	6
1.3.1.5	Drug models	7
1.3.2	Genetic models.....	7
1.3.2.1	LRRK2 transgenic and knock-out (KO) models	7
1.3.2.2	KO rat models of recessive genes.....	8
1.3.3	aSyn transgenic and adeno-associated viral (AAV)-mediated models.	9
1.4	Anatomy of basal ganglia (BG)	10
1.4.1	Direct and indirect pathway	10
1.4.2	Nigrostriatal pathway	12
1.5	Neurodegeneration	12
1.5.1	Pro- and antidegeneration markers	12
1.5.2	Nrf2 and oxidative stress.....	13

1.5.3	Tau and protein misfolding	15
1.5.4	NMNAT2 and axonal protection.....	16
1.5.5	SARM1 and axonal degeneration	17
1.6	Aim of the study	18
2	Material and methods	20
2.1	Animals	20
2.2	Material	20
2.2.1	Behavioral tests	20
2.2.2	Stereotaxic injection	20
2.2.3	Tissue processing.....	21
2.2.4	Stainings.....	21
2.2.4.1	Reagents	21
2.2.4.2	Antibodies.....	21
2.2.5	Softwares and equipments.....	21
2.3	Chemical and solution list.....	22
2.4	Chemical and solution preparation	23
2.5	Behavioral tests	23
2.5.1	Cylinder test.....	23
2.5.2	Pellet-reaching task	24
2.6	Stereotaxic injection of AAV1/2 serotype	25
2.6.1	Preparing solutions for injection	25
2.6.2	AAV1/2 injection.....	25
2.7	Tissue processing.....	26
2.7.1	Horizontal 10° fresh frozen sections	26
2.7.2	Coronal free-floating sections	27
2.8	Immunohistochemistry	27
2.8.1	Tyrosine hydroxylase (TH) staining.....	27

2.8.2	TH/Nissl staining	28
2.8.3	TH/aSyn immunofluorescence double staining	28
2.8.4	Immunofluorescence double staining of TH and pro- and antidegeneration markers	29
2.9	Unbiased stereology for SN neurons.....	29
2.10	Image processing	30
2.10.1	Optical density analysis of TH+ dopaminergic axons and TH+ dopaminergic fibers in the striatum.....	30
2.10.2	Cell counting of TH+ DA neurons.....	30
2.10.3	Immunofluorescence intensity analysis of pro- and antidegeneration markers.....	30
2.11	Statistical analysis	31
3	Results.....	32
3.1	The nigrostriatal tract is best visible in horizontal 10° sections.....	32
3.2	Verification of AAV1/2-A53T-aSyn injection in the rat SN	32
3.3	Time-dependent progressive motor impairment of the contralateral paw in the AAV1/2-A53T-aSyn PD rat model.....	34
3.4	Time-dependent progressive neurodegeneration of nigrostriatal dopaminergic tract in the AAV1/2-A53T-aSyn PD rat model.....	36
3.5	Time-dependent progressive loss of TH/Nissl+ SN neurons in the AAV1/2-A53T-aSyn PD rat model.....	37
3.6	Progressive motor deficits correlate with striatal dopaminergic denervation but not with dopaminergic perikarya loss in the AAV1/2-A53T-aSyn PD rat model.....	39
3.7	Downregulation of Nrf2 expression in the nigrostriatal perikarya and TH-immunoreactive axons of the AAV1/2-A53T-aSyn PD rat model.....	40
3.8	A trend of nonsignificant Tau downregulation in the nigrostriatal perikarya and nonsignificant upregulation in the TH-immunoreactive axons of the AAV1/2-A53T-aSyn PD rat model	42
3.9	No evident alterations of SARM1 expression in the nigrostriatal tract of the AAV1/2-A53T-aSyn PD rat model.....	

3.10	No evident alterations of NMNAT2 expression in the nigrostriatal tract of the AAV1/2-A53T-aSyn PD rat model.....	47
4	Discussion	49
5	Conclusion	57
6	Reference.....	60
7	List of figures and tables.....	71
8	Abbreviations.....	72
9	Note of thanks	74

1 Introduction

1.1 Parkinson's disease (PD)

Parkinson's disease (PD) is the second most common neurodegenerative disease in the world. It is a progressive and chronic movement disorder with symptoms of rigidity, resting tremor, postural instability and bradykinesia, predominantly affecting elderly people. PD patients also suffer from non-motor symptoms such as depression and sleep disturbances. Approximately 2% of individuals over 65 years and 4%-5% of individuals over 85 years are affected by this prevalent disease (Eriksen et al. 2003). The most critical pathophysiological hallmark of PD is loss of dopaminergic (DA) neurons in the substantia nigra pars compacta (SNpc) of the brain. Degeneration of the DA neurons lead to abnormal activities of basal ganglia that finally result in a series of motor dysfunction. Another crucial hallmark of PD is accumulation of Lewy bodies (LBs) that mainly consist of alpha-synuclein (aSyn), a protein whose pathophysiological role remains to be understood. A few studies assume that aSyn is tightly correlated with presynaptic vesicles and that it influences synaptic transmitter release (Bottner et al. 2015). Evidence has also been shown that aSyn toxicity may cause DA neuron damage in the SN and dystrophic neurites of DA neurons (Chu et al. 2016, Neumann et al. 2004). Until now, there is no causal therapy for PD available.

1.2 Etiology of PD

In spite of enormous seeking to understand the pathogenesis of PD, the exact mechanism still remains elusive (Pezzoli & Cereda 2013). Except for a few rare heritable PD cases, most of them occur in a sporadic manner (Chai & Lim 2013). It is plausible that sporadic forms of PD appear as a confluence of environmental and genetic factors (Cacabelos 2017).

1.2.1 Environmental factors

The incidence of PD is affected by factors such as age (Collier et al. 2011), gender (Lubomski et al. 2014) and ethnicity (Pringsheim et al. 2014, Van Den Eeden et al. 2003, Wright Willis et al. 2010). Meanwhile, numerous environmental toxins (Di Monte 2003),

occupational exposure to chemicals (Gamache et al. 2017, Pezzoli & Cereda 2013) and rural residency (Peters et al. 2006), etc. may contribute to some PD cases (Ball et al. 2019).

1.2.2 Genetic causes

Familial forms of PD are caused by either autosomal dominant or autosomal recessive mutations (Lill 2016). Autosomal dominant genes include mutations in LRRK2 and SNCA while Parkin, DJ1-PARK7 and PINK1 are involved in recessive mutations. Among the large body of candidate genes studied, LRRK2, SNCA, Parkin, PINK1 and DJ1 are best investigated. These genes might be causative in familial forms of PD (Kim & Alcalay 2017).

1.2.2.1 SNCA

The first gene that is linked to familial PD is the SNCA gene, which is also the first mutation gene identified in PD in 1990 (Golbe et al. 1990). The SNCA gene encodes aSyn protein and corresponds to the chromosomal loci of PARK1 and PARK4. SNCA has been reported to be the primary causative gene resulting in the early onset of familial Parkinson's disease (FPD) (Siddiqui et al. 2016). Duplication/triplication of the wild type (wt) SNCA can lead to familial, autosomal dominant forms of PD (Chartier-Harlin et al. 2004, Singleton et al. 2003), implying that aggregates of normal aSyn protein are sufficient in the disease induction of PD.

Point mutations are in charge of altering the amino-acid sequence of the aSyn protein, thus causing rare, autosomal dominant inherited forms of PD (Abeliovich & Gitler 2016, Polymeropoulos et al. 1996). Five missense mutations in the SNCA gene have been identified up to now, i.e., A30P (Kruger et al. 1998), E46K (Zarranz et al. 2004), H50Q (Appel-Cresswell et al. 2013), G51D (Lesage et al. 2013) and A53T (Polymeropoulos et al. 1997). Except for missense mutations of SNCA, common genetic variants (defined as being found in over 1% of a population) at SNCA locus (Abeliovich & Gitler 2016), including single nucleotide polymorphisms (SNPs), also add to the risk of developing PD (Nalls et al. 2014, Nalls et al. 2011). Studies suggest that the effect of SNPs attribute to modification of gene expression, rather than alteration of protein-coding sequences (Rhinn et al. 2012, Soldner et al. 2016).

Furthermore, in addition to familial forms of PD, SNPs in SNCA genes are associated with an increased possibility of developing sporadic PD (Cacabelos 2017).

aSyn is a 14.5 kDa, 140 a.a protein encoded by 5 exons in SNCA gene and it is a presynaptic protein that is discovered to be the building blocks of LBs, the pathological hallmark of PD (Lee & Trojanowski 2006, Spillantini et al. 1997). This protein is expressed not only in SN (Kim et al. 2004), hippocampus and neocortex in the brain predominantly presynaptic terminals, but also in heart, skeletal muscle and pancreas (Hashimoto & Masliah 1999, Lucking & Brice 2000). The physiologic cellular function and metabolic pathways of aSyn still remain ambiguous, with studies considering its role in regulating dopamine release and transport, due to its relationship with the synaptic vesicles. In addition, it gives rise to the fibrillization of the microtubule protein and plays the function of inhibiting p53 expression, which results in a neuroprotective effect in non-dopaminergic neurons (Costa et al. 2000, Tang et al. 2008). Nevertheless, this protection could not be observed on missense mutations (especially A53T) of SNCA with explanations that aggregations of misfolded aSyn increase the expressions of p53 and promote apoptosis (Costa et al. 2000). Moreover, it has been documented that oxidatively modified SNCA is more vulnerable to aggregate than native protein (Siddiqui et al. 2016), and that A53T mutation of SNCA accounts for an increase in endoplasmic reticulum(ER) stress and mitochondrial depolarization which lead to cell death (Smith et al. 2005).

1.2.2.2 LRRK-2

LRRK-2 gene involves six types of pathogenic mutations, the most common of which is named Gly2019Ser, which has a mutation frequency of 1% in sporadic PD and 4% in hereditary Parkinson's syndrome (Healy et al. 2008, Paisánruíz et al. 2004). The clinical manifestations are similar to sporadic PD, however with a more benign disease course and low possibility of developing dementia. The probability of developing Parkinson's syndrome in people under 60 years of age with Gly2019Ser mutation is 28%, while the percentage in 79-year-olds rises to 74% (Healy et al. 2008).

1.2.2.3 Recessive genes

Mutations in the Parkin, PINK1 and DJ-1 genes can cause recessive early-onset Parkinsonism. The onset of the disease is under 40 years of age. Patients are manifested by abnormal gait, resting tremor of the lower extremities, and early behavioral abnormalities (Williams et al. 2005). The first mutation in the gene for the Parkin protein (PRKN) was described in 1998 (Hattori et al. 1998), while PINK1 gene was first discovered in three European families with PD (Funayama et al. 2008, Marongiu et al. 2008), Parkin gene is one of the best-studied genes in the analysis of the etiology of PD (Anna et al. 2013). Parkin is an ubiquitin ligase functioning in the ubiquitin-proteasome system. It is believed defects in the function of ubiquitin protease to degrade proteins lead to aggregation of toxic proteins which are closely related to mutations in aSyn and Parkin genes (Olanow & Mcnaught 2006).

Both PINK1 gene and Parkin gene lead to disease induction via the mitochondrial pathway (Clark et al. 2006, Park et al. 2006). Loss of mitochondrial function is the primary cause of autosomal recessive Parkinsonism (Schapira 1994). What is more, it is known that PINK1 interacts with PARKIN and DJ1 (Plunfavreau et al. 2007). DJ1 protein is a hydroperoxide reactive protein involved in oxidative stress. The functions of DJ-1 protein are impaired after DJ-1 gene mutation, which increases the damage of neurons caused by oxidative stress (Plunfavreau et al. 2007).

1.3 Animal models of PD

Despite the fact that currently there is not yet a perfect animal model which depicts thoroughly motor and pathological features of human PD system, a variety of well-established animal models, especially with rodents, has been frequently adopted to promote understanding of the characteristics of PD.

1.3.1 Neurotoxic models

1.3.1.1 6-hydroxydopamine (6-OHDA) model

The 6-OHDA model is produced by 6-OHDA forming hydroxyl radicals and inhibiting mitochondrial respiratory chain complexes I and IV, which leads to selective loss of DA

neurons, resulting in symptoms characteristic of PD. The disadvantages of this model are:

a. 6-OHDA cannot pass the blood-brain barrier (BBB), thus should be stereotaxically injected into the substantia nigra, the medial forebrain bundle or the striatum (Przedborski et al. 1995) which lowers the success rate of model induction. As a result, this model has certain limitations in the selection of model animals, therefore rats are most suitable while smaller animals e.g. mice are not considered to be an ideal model for 6-OHDA.

b. DA neurons begin to degenerate within 24 hours after 6-OHDA injection, and striatal dopamine decreases significantly after 2 to 3 days (Faull & Lavery 1969). Therefore, this model only produces acute effects, which is substantially different from the pathological features of chronic and age-dependent progression of human PD.

c. 6-OHDA model is not able to produce aggregation of LB, which is the pathophysiological symbol of PD (Schober 2004), so it is impossible to accurately mimic PD characteristics.

In summary, the 6-OHDA model is not the most ideal PD animal model.

1.3.1.2 MPTP model

The mechanism of the MPTP model is that MPTP is modified to its metabolite – an active substance called 1-methyl-4-phenylpyridinium (MPP⁺) after binding to monoamine oxidase B in the brain. MPP⁺ will be specifically taken up into DA neurons via the dopamine transporter, and then transported into mitochondria, thereby inhibiting the activity of mitochondrial complex I, leading to degeneration and apoptosis of DA neurons (Javitch et al. 1985, Tipton & Singer 1993). The advantages and disadvantages of this model are as follows:

a. Non-human primates such as monkeys are very susceptible to MPTP. Moreover, the biochemical and cellular alterations induced by MPTP in monkeys are very similar to those of PD patients, and the MPTP PD monkey models can be evaluated in behavioral, and mental disorders (Dauer & Przedborski 2003, von Bohlen Und Halbach 2005).

However, due to economic and ethical restrictions, etc., primate models have only been used in a few laboratories around the world (Cenci et al. 2002).

b. MPTP is highly lipophilic and can easily penetrate the blood-brain barrier, so the administrative methods are variable (percutaneous, intraperitoneal, intravenous or intramuscular injection) (Przedborski et al. 2001) and easily accessible as compared to brain injection.

c. Rats are not sensitive to MPTP (Bove et al. 2005), while mice respond to MPTP toxicity well though slightly worse compared with primates (Bove et al. 2005). Besides, mouse models mimic the biochemical and cellular features of human PD (von Bohlen Und Halbach 2005). However, the behavioral defects of MPTP mouse models are almost entirely reversible (Przedborski et al. 2001).

The MPTP model is one of the most ideal PD animal models and has been widely used in the experimental research of PD.

1.3.1.3 Rotenone model

Rotenone is an insecticide that has a damaging effect on the central DA nervous system. This substance selectively impacts the nigrostriatal dopaminergic pathway and causes oxidative stress damage in the striatum, thus possibly simulating the pathogenesis of PD (Betarbet et al. 2000).

The rotenone model has been widely used in exploring the pathogenesis and treatments of PD. Usually, this model reproduces many features of PD including nigrostriatal degeneration, behavioral deficits and LB morphology (Betarbet et al. 2000, Pan-Montojo et al. 2010, Sherer et al. 2003). However due to the high toxicity of rotenone, the mortality of rotenone animal models is high which eliminates the use of this model.

1.3.1.4 Herbicide (Paraquat) model

Paraquat is able to come across the BBB and lead to DA cell damage and motor impairment of the animals. However, the way that herbicide exposes in the environment are somehow distinct from those actual environmental factors, and the survival rate of animals after Paraquat injection is low. Since the mechanisms of the toxic effect of

Paraquat still remains vague (Melrose et al. 2006), further research is needed for this model.

1.3.1.5 Drug models

Reserpine is an inhibitor drug for the adrenergic nervous system which suppresses dopaminergic system. Reserpine binds to the recognition site of the dopamine vesicle transporter irreversibly, resulting in toxic metabolites of dopamine, which results in high expression of p53 and in turn induces apoptosis in DA cells, and eventually causes symptoms such as static tremor and bradykinesia similar to PD (Jiang et al. 2004). Nonetheless, as the effect of reserpine is transient without morphological changes of DA neurons, and because of the fact that large doses of reserpine produce drug toxicity, reserpine is not used as a usual substance to induce PD models. However, this model is absolutely sufficient for research purposes in treatment effect of DA substitutes e.g. L-DOPA and dopamine agonists (Leao et al. 2015).

1.3.2 Genetic models

The discovery of genetic mutations such as aSyn, parkin, ubiquitin C-terminal hydrolase L1, LRRK2, PINK1 and DJ-1 which causally linked to PD (Wood-Kaczmar et al. 2006) led to development of genetic animal models of PD, which allows us to better understand PD regardless of the high requirements for technical skills and huge cost in generating genetic animal models. Although the behavioral phenotypes of genetic models are usually rather distinct from human cases, quite a few cellular and molecular defects have been proven to attribute to gene mutations (Blesa & Przedborski 2014, Exner et al. 2012, Gandhi et al. 2009, Ottolini et al. 2013).

Mice were more frequently used to generate transgenic PD models because mutagenesis is more accessible in mice. However in recent years with technology advances in genome engineering and viral vectors, rats have been increasingly used for transgenic models and viral vector-induced overexpression or mutations of genes of PD (Creed & Goldberg 2018).

1.3.2.1 LRRK2 transgenic and knock-out (KO) models

LRRK2 KO rats failed to show either dopaminergic loss of neurons in SN or motor impairment which are characteristic of PD (Daher et al. 2014). The lines of transgenic

rats have been largely studied (Lee et al. 2015, Shaikh et al. 2015, Sloan et al. 2016, Walker et al. 2014). No transgenic rats show significant loss of dopaminergic cells, but for behavioral phenotypes much evidence were found (Sloan et al. 2016). For instance, Walker et al. documented that LRRK2 rats which overexpress human G2019S showed impaired movement in rota rod test (Walker et al. 2014). Moreover, Sloan reported the BAC transgenic rats which express human G2019S or with R1441C mutations in the LRRK2 gene developed behavioral defects (Sloan et al. 2016). However, despite some behavioral evidence, neither LRRK2 KO rats nor LRRK2 transgenic rats are considered to be ideal models for PD because of the lack of showing pathological hallmarks of PD.

1.3.2.2 KO rat models of recessive genes

In comparison to PINK1 KO mice, rats models with knock out in the PINK1 gene displayed distinct advantages in mimicking age-dependent loss of dopaminergic neurons in SN at the stage of 6-8 months (Dave et al. 2014, Villeneuve et al. 2016) and behavioral deficits (Dave et al. 2014, Grant et al. 2015) at the age of 4 months. Moreover, aSyn aggregates (Grant et al. 2015, Villeneuve et al. 2016) and non-motor abnormalities like critical age-dependent vocalization deficits (Grant et al. 2015) have also been described for PINK1 knock-out rats. All the above merits of the PINK1 knock-out rat model are not found in most other genetic animal models (Creed & Goldberg 2018). For this reason, this recently developed rat model may be notably helpful for exploring therapeutic methods to prevent age-dependent pathological alterations.

DJ-1 KO rats displayed a significant progressive loss of DA neurons from 6 to 8 months of age (Dave et al. 2014), accompanied by motor deficits and reduced dopamine in the striatum (Dave et al. 2014, Sun et al. 2013). This relatively new rat model has been successfully recruited in investigating neuroprotective compounds, e.g. an HDAC inhibitor has been found to relieve motor impairment and apoptosis in DJ-1 KO rats (Chiu et al. 2013).

Unlike PINK1 and DJ-1 KO rats, Parkin KO rats show no distinctive symbols of PD, inclusive of behavioral defects, loss of DA neurons (Dave et al. 2014) and aggregation of Lewy body (Doherty & Hardy 2013). Nonetheless, some researchers have reported that this Parkin KO rat models are favorable to proteomic studies and examining substrates

of Parkin, thus might be helpful to explore cellular and molecular mechanisms of PD (Kurup et al. 2015, Stauch et al. 2016).

1.3.3 aSyn transgenic and adeno-associated viral (AAV)-mediated models

Mice and rats have been frequently used to generate aSyn transgenic or wt-aSyn overexpressing models (Koprach et al. 2017, Lee et al. 2012). There are rat lines overexpressing human aSyn which mimic key aspects of PD. For example, BAC transgenic rats overexpressing wt human-aSyn have shown significant loss of DA neurons at the age of 18 months and decreased striatal dopamine level together with motor impairment at the age of 12 months (Nuber et al. 2013).

In recent years AAV vectors have been largely made use of in generating exogenous aSyn. Rats are more often used for AAV delivery because AAV delivery requires high accuracy of injecting into a rather tiny structure in SNpc (Kirik et al. 2002, Klein et al. 2002). In comparison with transgenic aSyn models, AAV-mediated aSyn models display a progressive, age-dependent nigrostriatal degeneration and behavioral dysfunction within a shorter time period (Kirik et al. 2002, Klein et al. 2002). Most importantly, Lewy body or Lewy neurites primarily composed of aSyn as a hallmark of PD are clearly visualized in the AAV-mediated aSyn model. In addition, AAV vectors can be unilaterally injected into the brain, which allows for using the uninjected side of the brain as a standardized control for examining histological stainings and paw asymmetry in behavioral test.

A large body of research has combined the genomic elements of AAV serotype 2 with capsid proteins from AAV serotypes 1, 2, 5, 6, 7, 8 or 9, with the purpose of promoting aSyn expression (Bourdenx et al. 2015, He et al. 2016, Van der Perren et al. 2015, Yamada et al. 2005). In 2010, Koprach et al. combined the AAV serotype 2 with AAV serotype 1 to generate a new PD rat model which has both the distinct advantages of serotype 2 (specific neuronal tropism, ability to achieve high purity and high titer) and serotype 1 (distinguished ability to penetrate brain tissue) (Koprach et al. 2010). AAV serotype 1 and AAV serotype 2 were expressed in a ratio of 1:1 on the viral capsid which could drive the expression of human-mutated A53T gene (Koprach et al. 2010). In this model, significant degeneration of nigrostriatal tract and accumulation of aSyn were

detected within 3 weeks after unilateral injections of AAV1/2 in SN of the rat brain (Koprach et al. 2010). The short time course of developing key pathologies of PD preserves time and consume.

Later in one study conducted by Musacchio et al., severe motor defects, significant nigrostriatal degeneration as well as specific aSyn aggregates have developed 6 weeks after unilateral AAV1/2-A53T-aSyn injections into the SN of rat brain (Musacchio et al. 2017). However up till now, little attention has been paid to the clinical and pathological alterations on this AAV1/2-A53T-aSyn model at earlier time points.

1.4 Anatomy of basal ganglia (BG)

Basal ganglia (BG) refer to a series of subcortical nuclei derived from the telencephalon. BG is mainly composed of four related nuclei: striatum (STR), globus pallidus (GP), SN and subthalamic nucleus (STN). These nuclei are deeply located in the brain between two hemispheres, establishing a complex network to deal with information from cortex, about motor control and learning, etc.

1.4.1 Direct and indirect pathway

PD is characterized by abbreviate neuronal activity in BG. Traditional theory holds that there are two main pathways in the basal ganglia network: the direct pathway and the indirect pathway (Figure 1).

The direct pathway is: cerebral cortex → STR (input nucleus) → internal globus pallidus (GPi), substantia nigra pars reticulata (SNpr) (output nucleus) → thalamus (THA) → cerebral cortex. The neurotransmitter from the cerebral cortex to STR is glutamate which is excitatory. And neurotransmitters from STR to GPi or SNpr are inhibitory gamma-aminobutyric acid (GABA) and substance P. It is also GABA, which plays the role of inhibitor from GPi or SNr to THA. Then excitatory projection from THA to the cortex is emitted. When the cortex sends an excitatory signal to the STR, which in turn inhibits the suppressor cells in the GPi or SNr, THA is activated, finally activating the motor cortex.

The indirect pathway is: cerebral cortex → STR → GPe → STN → GPi, SNr → THA → cerebral cortex. GABA acts as an inhibitory neurotransmitter from STR to GPe and from

GPe to STN. The neurotransmitter from STN to GPi or SNr is glutamate. So, when STR is activated by cortex, which would inhibit GPe, fewer inhibitory signals from GPe to STN would be sent. As a result, disinhibition of STN takes place which excites GPi and SNr. At last, THA would be suppressed and cortex would be less activated, thus preventing excessive movement.

Under normal conditions, the direct and indirect pathways are in equilibrium, working together to produce controlled movements. The aforementioned is a highly simplified summary of the basal ganglia network, ignoring several other pathways, such as the hyperdirect pathway which transports cortical information directly to STN (Bosch et al. 2012). In fact, the neural network constructed by the basal ganglia is much more complicated than generally understood.

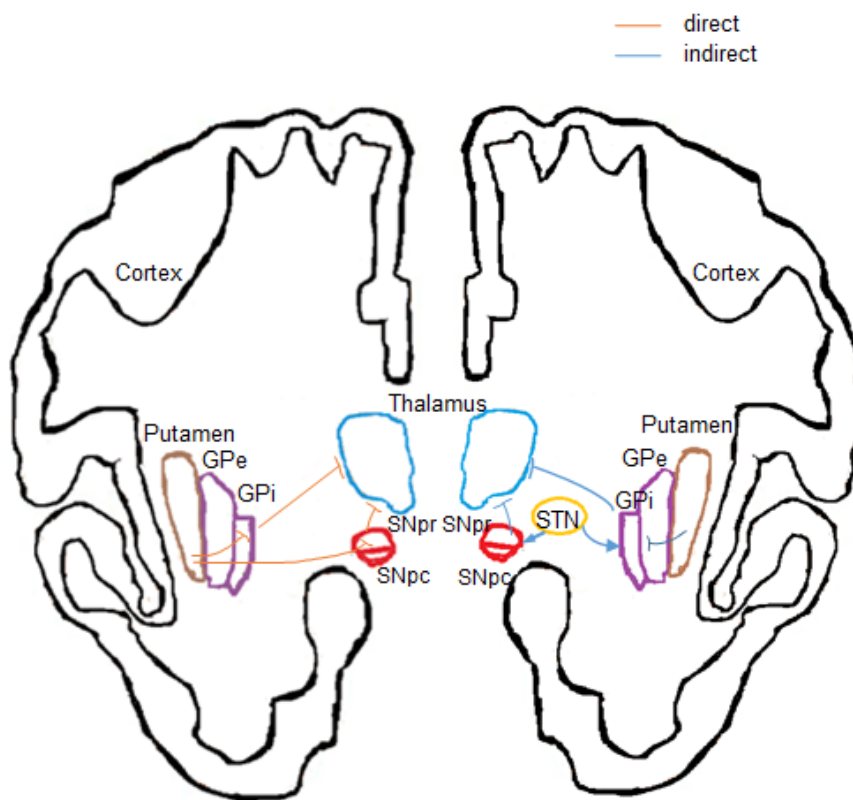


Figure 1: Schematic illustration of the direct and indirect pathway in the basal ganglia network.

SNpr: substantia nigra pars reticulata, SNpc: substantia nigra pars compacta, STN: subthalamic nucleus, Gpi: internal globus pallidus , Gpe: external globus pallidus.

1.4.2 Nigrostriatal pathway

The nigrostriatal pathway is a dopaminergic pathway that connects the SNc with the STR. It is one of the four major dopaminergic pathways in the brain and it is essential in the production of movement as part of BG. The nigrostriatal tract consists of SN, dopaminergic axons and STR. DA is transmitted from SN to STR as a neurotransmitter. Lack of DA in the nigrostriatal pathway affects movement, muscle control, and balance. DA also plays a role in the body's motivation and reward mechanism in other neuropathways in the brain.

It is the nigrostriatal system, which maintains the balance of direct and indirect pathway. DA neurons of this pathway release DA through dopaminergic axons to GABAergic medium spiny neurons in the STR. In physiological state, DA projecting from SNpc to STR can excite D1 receptors in STR which are excitatory and inhibit D2 receptors which are inhibitory in STR, thus exerting excitatory effects on the direct pathway and suppressive effects on the indirect pathway. In PD case, degeneration of the nigrostriatal tract leads to a decrease of DA release and excitability of the D1 receptor in STR, which in turn reduces the excitability of the direct pathway. At the same time, the repressive influence of DA transmitter from SN on D2 receptors in STR is reduced, resulting in disinhibition of indirect pathways. With combined impacts of these two pathways, movement symptoms such as tremor, rigidity and dyskinesia occur.

1.5 Neurodegeneration

1.5.1 Pro- and antidegeneration markers

Neurodegeneration is age-dependent and characterized by progressive loss of neuronal structures or functions. It plays an essential role in neurodegenerative diseases, such as PD, Alzheimer's disease (AD) and multiple sclerosis. These diseases are incurable as a result of degeneration of neurons (Gitler et al. 2017). The cellular and molecular mechanisms of neurodegeneration include oxidative stress (Liu et al. 2017, Wang et al. 2017), mitochondrial damage (Lin & Beal 2006), protein aggregates (Zarranz et al. 2004) and axonal transport (De Vos et al. 2008) and so on (Figure 2).

There is a series of molecules associated with neurodegeneration, which have been reported as “pro- and antidegeneration markers” , indicating they might participate in the degeneration process in neurodegenerative diseases. Among them some crucial factors have been frequently studied in recent years, such as SARM1, Tau, Nrf2 and NMNAT2. For instance, Ramsey et al. reported that Nuclear Factor Erythroid 2-Related Factor 2 (Nrf2) mediates pathogenic process in AD and PD through antioxidant defense (Ramsey 2007, Hayes & Dinkova-Kostova 2014).

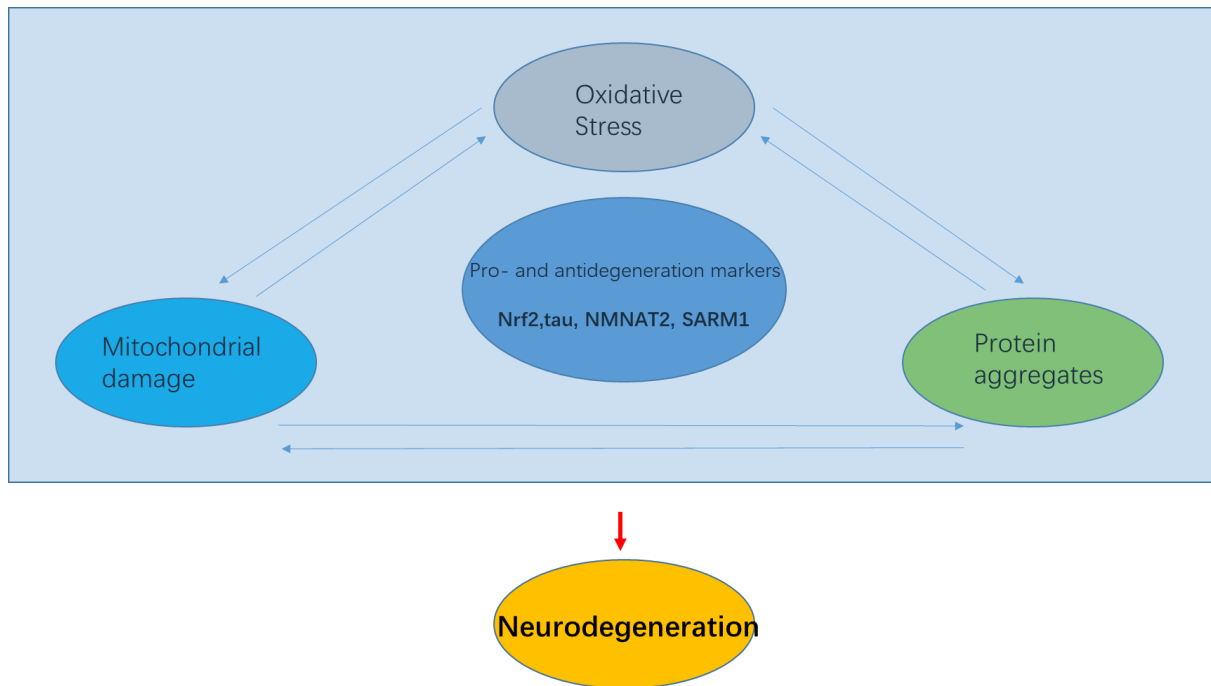


Figure 2: Schematic image of multiple pathogenesis of PD.

1.5.2 Nrf2 and oxidative stress

Oxidative Stress (OS) refers to a disturbance in the balance between oxidation and anti-oxidation. Excess oxidation leads to inflammatory infiltration of neutrophils, increased secretion of proteases, and a large number of oxidative intermediates. Oxidative stress is a negative process produced by free radicals and it is considered to be an essential factor in aging and disease (Burton & Jauniaux 2011). The brain is particularly sensitive to oxidative stress (Cobley et al. 2018). Under pathological conditions, OS leads to a significant increase in reactive oxygen species (ROS) levels in the central nervous system. However the antioxidant capacity is limited, resulting in oxidative damage in neurons (Garbarino et al. 2015). Oxidative damage is a common feature of a large number of neurodegenerative diseases (Love 1999). For instance, increased ROS production during

oxidative stress leads to degeneration of DA neurons in the brain, which is suggested to be the key mechanism of neurodegeneration in DA neurons (Jenner 2003).

Nrf2 is a transcription factor involved in fighting against cellular OS and it plays a major regulatory role in many genes, involving genes related with antioxidant, anti-inflammatory pathways (Alfieri et al. 2011). Under physiological circumstances, Nrf2 binds to cytoskeleton-associated protein Keap1 in the amino-terminal Neh2 domain and presents in the cytoplasm in the form of a dimer, so that the antioxidants are able to stay at the basal expression level, which keeps cells in a stable state (Alfieri et al. 2011). Under OS, the body is attacked by oxygen free radicals and endogenous toxins which dissociate Nrf2 and Keap1 and lead to the translocate of Nrf2 into the nucleus (Itoh et al. 1999). Nrf2 binds the antioxidant reaction elements (ARE) in the nucleus and activates downstream target genes, which can regulate the expression of antioxidant proteins (Johnson et al. 2008). This Nrf2 antioxidant pathway - Nrf2 / ARE pathway is the most important endogenous antioxidant pathway (Johnson et al. 2008). Besides, it is said that Nrf2 encompasses a nuclear export sequence which removes Nrf2 from the nucleus into cytoplasm when the balance between oxidation and anti-oxidation is achieved. Another study conducted in patients of demyelination by a has reported that axonal damage may lead to nuclear transport of Nrf2 into cytoplasm which results in aberrant function due to impaired response to OS, and nuclear retention of Nrf2 under OS is essential for transcription of genes responsible for anti-oxidative defense (Haines et al. 2015).

As the key factor in regulating oxidative response, Nrf2 is considered to play an essential role in fighting against oxidative damage in PD (Ahuja et al. 2016). Nrf2 is mainly present in the cytosol of DA neurons in SN, and the presence of Nrf2 in the nucleus of early PD patients suggests its attempts to reduce oxidative stress (Ramsey et al. 2007). Meng et al. have stated that Nrf2 expression in DA neurons was decreased in the MPTP PD rat model, and stronger expression of Nrf2 as well as less damage of DA neurons were observed after matrine treatment which was supposed to inhibit the oxidative damage (Meng et al. 2017).

Contrary to this study, Ramsey et al. have found in their experiment that Nrf2 nuclear staining in DA neurons in SN is abundantly stronger as compared to control groups

(Ramsey 2007). However this phenomenon was only observed in the surviving neurons which may indicate that nuclear translocate of Nrf2 to the nucleus may delay death of the surviving neurons. In the neurons which have been lost, Nrf2 protection may not be sufficient probably due to insufficient transport of Nrf2 into the nucleus. All in all, Nrf2 is considered to have neuroprotective effects on PD animal models (Dringen et al. 1999) by significantly alleviating oxidant damage caused by some pathogenic factors (MPTP, rotenone, or hydrogen peroxide in vitro and in vivo). DA neurons are protected by antioxidant enzymes whose transcription are regulated by Nrf2 (Itoh et al. 2003). These studies suggest that defects in Nrf2 regulation in antioxidant responses may play a role in PD, and nowadays Nrf2 is regarded as a valuable treatment target to evaluate the efficacy of oxidative stress regulation. However, further research is still needed.

To date studies focusing on the mechanisms of Nrf2 function in PD are still rare, the regulation of Nrf2 expression in PD and its nuclear transport under physiological conditions and OS still remains to be explored. What is more, there have been some discrepant findings stated above.

1.5.3 Tau and protein misfolding

Microtubules are one of the main skeleton components of neurons, composed of tubulin proteins and microtubule-associated proteins (MAP) (Riederer et al. 1995). Tau protein is an MAP whose primary biological function is to maintain formed microtubules and promote protein assembly (Shaw-Smith et al. 2006). Tau protein is mainly located in neurons and also expressed in a small amount in astrocytes and oligodendrocytes (Shin et al. 1991). Physiologically, Tau protein contains 2-3 phosphate groups, and its phosphorylation level is regulated by protein kinase and protein phosphatase (Alonso et al. 2001). In physiological state, Tau protein is phosphorylated to a certain degree, and the phosphorylated Tau is soluble and unfolded. Tau is tightly associated with the development of neurons, such as cell growth and migration (Zhang et al. 2018). Nonetheless, hyperphosphorylation leads to tau misfolding and aggregation, which separates Tau protein from microtubules (Arai et al. 2001). As a result, cytoskeleton structure and function of neurons are directly damaged (Arai et al. 2001). There has

been increasing evidence that Tau protein and p-tau protein are involved in neuron death (Armstrong & Cairns 2013).

Tau is considered as a key protein involved in a few neurodegenerative diseases, especially in AD (Brion et al. 1985). One of the primary pathological hallmarks of AD is the neurofibrillary tangle composed of Tau (Galpern & Lang 2006). Studies have shown that AD-like pathology in the brain of PD patients has greatly promoted cognitive impairment in PD (Irwin et al. 2013). About 33% of PD patients with dementia are associated with AD-like pathological manifestations (Irwin et al. 2016). Tau is indicated to be closely linked with sporadic PD by a genome-wide association study and tauopathies is observed in 50% of PD cases (Zhang et al. 2018). Tau and aSyn have been largely reported to interact and promote each other under pathological conditions (Wills et al. 2010). Co-existence and enhanced levels of p-tau and aSyn have been found in neuronal LBs in a PD mouse model (Wills et al. 2010). Distinct to the widespread tau expression in the entire brain in AD, tauopathies in PD patients and PD patients with dementia have only been detected in DA neurons (Jellinger 2011).

Although tau pathology has been previously described in neurodegenerative diseases, particularly in AD, its role and importance in PD have been undervalued.

1.5.4 NMNAT2 and axonal protection

Nicotinamid mononucleotide adenylyltransferase (NMNAT) is an enzyme that catalyses nicotinamide adenine dinucleotide (NAD) synthesis which is crucial for axonal survival (Conforti et al. 2014). NMNAT family contains three isoforms in mammal, including NMNAT1, NMNAT2 and NMNAT3 which are named by distinct properties and structure distributions (Di Stefano & Conforti 2013). NMNAT1 is mainly localized in the nucleus and it is in charge of neuronal survival (Koenekoop et al. 2012); NMNAT2 is located cytoplasmic and axoplasmic, and is abundant in the brain (Conforti et al. 2014, Gilley et al. 2013). It has been emphasized on bidirectional axonal transport and responsible for axonal growth and survival (Gilley & Coleman 2010, Hicks et al 2012; another family member NMNAT3 is probably expressed in mitochondria (Conforti et al 2014). Among these three NMNAT isoforms, NMNAT2 has been largely valued for the fact that it plays an essential role in both Wallerian degeneration after injury (Fang et al. 2012, Hicks et

al. 2012, Xiong et al. 2012) and Wallerian-like degeneration which is known as dying-back or retrograde degeneration (Bridi & Hirth 2018, Gilley & Coleman 2010). Similar to the slow Wallerian degeneration protein which contains NMNAT1, NMNAT2 overexpression relieves Wallerian degeneration (Milde et al. 2013) whereas removal of endogenous NMNAT2 would lead to axonal degeneration (Gilley et al. 2013, Hicks et al. 2012). The effect of NMNAT2 on Wallerian degeneration benefits from its enzymatic activity in synthesizing NAD (Conforti et al. 2014). However the role of NMNAT2 in Wallerian-like degeneration in uninjured axons is independently from its enzymatic function of synthesizing NAD (Ali et al. 2016). Recently, NMNAT2 has been newly identified as a protective protein in inhibiting the aggregates of the pathological proteins to delay the dying-back axonal degeneration in a few neurodegenerative diseases, including AD (Liang et al. 2008) and PD (Lesnick et al. 2007). For instance, in AD brains the NMNAT2 level decreased by 50%, and in humans the level of NMNAT2 is correlated with the level of cognitive impairment (Ali et al. 2016). Other studies have shown that NMNAT2 expression is downregulated and NMNAT2 mRNA levels declined in AD (Ali et al. 2016) and PD.

1.5.5 SARM1 and axonal degeneration

Sterile alpha and TIR motif containing 1 (SARM1) protein is an adaptor protein for Toll-like receptor and it contains the Toll-Interleukin-1 receptor domain involved in cell death or inflammation (Murata et al. 2013). SARM1 exerts a negative effect on Toll-Like receptor-activated transcriptional activities (Conforti et al. 2014). SARM1 has been reported to be preferentially expressed in neurons (Kim et al. 2007) and it is associated with neuronal toxicity and axonal degeneration in *Caenorhabditis elegans* (Chuang & Bargmann 2005) and mammals (Chen et al. 2011). SARM1 is best-known for its role as a pro-degeneration molecule in rapid Wallerian degeneration to trigger axonal degeneration after injury (Liu et al. 2014). Numerous reports have shown absence of SARM1 delays Wallerian degeneration to an extent (Conforti et al. 2014, Gerdtts et al. 2013, Osterloh et al. 2012). Moreover, in SARM1-knockdown mice motor deficit and electrophysiological response have been considered as an impact of SARM1 absence (Lin & Hsueh 2014). Interesting to mention is that SARM1 has been described as having a close relationship with NMNAT2 which is also one of our target molecules in this study

(Conforti et al. 2014, Gerdts et al. 2013) . In the study by Gerdts et al, SARM1 overexpression did not successfully induce axon degeneration without NMNAT2 loss, which was unexpected (Gerdts et al. 2013). Since SARM1 is widely distributed in different subcellular organelles, it also regulates different events such as innate immune response, apoptosis and neuromorphogenesis (Liu et al. 2014). Recently some studies have examined the association of SARM1 with PD (Murata et al. 2013). For example, Murata and colleagues reported that SARM1 together with TRAF6 stabilize PINK1 whose mutations cause autosomal recessive forms of PD and lead to mitochondria damage (Murata et al. 2013). Thus, it would be interesting to explore if SARM1 is also involved in our PD rat model and the mechanism behind it.

1.6 Aim of the study

A large body of the previous research about PD is established on neurotoxic models, with various or even contrasting observations in the aspects of behavioral performance, neurodegeneration of nigrostriatal tract or absence of pathophysiological symbol. In recent years an increasing number of in-vivo studies based on viral vector-induced animal models appear a lot of coincident outcomes have been confirmed from these models. Thus, we employed the AAV1/2-A53T-aSyn rat model in which behavioral and biochemical evidence with high reproducibility have already been characterized. Nowadays early intervention of disease process is recognized as critical and crucial as a result of unsatisfactory effect of current therapies which usually start at a late time point, usually after symptoms occur. Most earlier studies on the AAV1/2-A53T-aSyn rodent PD model focused on respectively late time points after disease induction, e.g. 6 weeks or 9 weeks (Ip et al. 2017, Koprach et al. 2010). In addition, up until now research has been largely focused on loss of DA cell bodies in SN, yet recently more researchers argue that axons and striatum of the dopaminergic tract are involved predominantly and early in PD (Tagliaferro et al., 2016). Undoubtedly, the absence of applicable and accurate therapeutic molecular targets also contributes to the unsatisfactory situation of treating PD. Although some crucial molecules associated with neurodegeneration (e.g. Nrf2, Tau, SARM1 and NMNAT2) have been studied in a few neurodegenerative disorders,

including PD, the exact mechanisms behind it still remains to be explored. Based on this background, the aim of this study is to address the following questions:

- i. Do motor impairments develop in a time-dependent pattern after disease induction in the AAV1/2-A53T-aSyn rat model?
- ii. When do pathophysiological changes and motor impairments begin to develop in the AAV1/2-A53T-aSyn rat model? Do pathological changes occur prior to motor deficits?
- iii. Where does the dopaminergic neurodegeneration of the nigrostriatal tract start?
- iv. Are there alterations of the pro- and antidegeneration markers (Nrf2, Tau, SARM1, NMNAT2) in the AAV1/2-A53T-aSyn rat model?

2 Material and methods

2.1 Animals

69 adult male wild-type Sprague-Dawley rats were purchased from Charles River Laboratories (Sulzfeld, Germany), and kept in a 12 hour/ 12 hour day/night rhythm with free food and water access. The weight of the rats is around 250g-270g.

All animal experiments were approved at the Regierung von Unterfranken (Würzburg, Germany). All guidelines regarding care, husbandry, and use of the animals were followed.

2.2 Material

2.2.1 Behavioral tests

Cylinder glass (diameter 20cm, height 30cm) custom made

Plexiglas box (length 34, width 14cm) custom made

2.2.2 Stereotaxic injection

5 µl microinjection syringe Hamilton Co., USA

isoflurane vaporizer Dräger AG., Germany

scalpel #10 Feather Co., Japan

suture materials (V97D9) Ethicon Inc., USA

Vet ointment Bepanthen, Germany

Rat stereotaxic frame, rat anesthesia mask, microinjection pump Stoelting
(Wood Dale, IL, USA)

oxygen, isoflurane, heating template, tissue forceps, electric razor, cotton swabs,
AAV1/2-A53T and AAV1/2-EV

2.2.3 Tissue processing

Bone scissors, PBS with heparin, needles, tissue pincers, brain matrix for rats, methylbutane, cryomodule, dry ice, cryostat, distilled water, object slides, cover slips, Aquatex (aqueous mounting media).

2.2.4 Stainings

2.2.4.1 Reagents

DAB-Peroxidase substrate solution kit	Vector Labs, USA
DAPI nuclear staining	Sigma-Aldrich, USA
ABC peroxidase standard staining kit	1:56, Thermo Fisher Scientific cat, USA

2.2.4.2 Antibodies

Rabbit anti-rat TH	Abcam, Cambridge, UK
Biotinylated goat anti-rabbit	Vector Laboratories cat, USA
Chicken-anti-rat TH	Abcam, UK
Mouse-anti-human aSyn	Invitrogen, USA
Goat-anti-chicken Cy3	Alpha Diagnostics cat, USA
Goat-anti-mouse Cy2 PA	Jackson ImmnoResearch Laboratories Inc., PA
DAPI nuclear stain	Sigma cat, USA
Rabbit anti rat Nrf2	GeneTex, USA
Rabbit anti rat Tau	Sigma, USA
Rabbit anti rat NMNAT2	Biorbyt, UK
Rabbit anti rat SARM1	MyBioSource, USA
Goat-anti-rabbit alexa fluor 488	Invitrogen, USA

2.2.5 Softwares and equipments

Graphpad Prism 7 software	San Diego, USA
---------------------------	----------------

Stereo Investigator software package	MicroBrightField Biosciences, USA
BX53 microscope	Olympus, Japan
NIH ImageJ software	LOCI, University of Wisconsin

2.3 Chemical and solution list

Isoflurane	CP-Pharma, Germany
Rimadyl	Zoetis, USA
Heparin	Rathiofarm, Germany
4% paraformaldehyde (PFA)	Merck, Germany
Sucrose	ROTH, Germany
2-Methylbutane	ROTH, Germany
OCT medium	Sakura, Germany
Normal bovine serum (BSA)	Sigma, Germany
Normal goat serum (NGS)	Dako, Germany
Hydrogen peroxide 30% (H ₂ O ₂)	Merck, Germany
Ethanol (EtOH)	Fischar, Germany
Sodium chloride (NaCl)	Sigma-Aldrich
Potassium chloride (KCl)	Merck, Germany
Hydrogen chloride (HCl, 1N)	Fluka, Germany
Glycerol	Merck, Germany
Paraformaldehyde (PFA)	Merck, Germany
Aqueous mounting media	Darmstadt, Germany
Xylene solution	St. Louis, USA
Aqua Polymount	Warrington, PA

Sodium hydroxide NaOH (5M)	Merck, Germany
Pap pen	Science Services, Germany
Sodium dihydrogen phosphate dihydrate (NaHPO ₄ x 2H ₂ O)	OTH, Germany

2.4 Chemical and solution preparation

10x (0.1 M) phosphate buffered saline (PBS): 80 g NaCl, 14.2 g NaHPO₄ x 2H₂O and 2 g KCl were dissolved in distilled water, then pH was adjusted to 6.8 with HCl.

1x (0.01 M) PBS: The 10x PBS solution was diluted with distilled water and pH was adjusted to 7.4.

PBS with heparin solution: for 60 ml 1x PBS, 0.2 ml heparin was added for perfusion of 1 rat.

Antifreeze cryoprotectant: consisted of 30% glycerol, 30% EtOH, 40% 0.01 M PBS.

30% sucrose solution: 30 g sucrose was dissolved in 100 ml 1 x PBS.

4% Paraformaldehyde (PFA): 10 g PFA was dissolved in 250 mL 0.01 M PBS and two drops of 5 M NaOH was added and solution was constantly stirred at 60°C. When PFA was resolved, pH was adjusted to 7.4 with HCl after the solution was cooled. Finally, the PFA solution was filtered.

10% BSA solution: 100g 0.1% BSA was dissolved in 100 ml 1x PBS and then filtered.

Blocking solution: composed of 2% normal bovine serum (BSA) and 10% normal goat serum (NGS) in 0.01 M PBS.

Diluent solution: composed of 2% BSA and 2% NGS in 0.01 M PBS.

2.5 Behavioral tests

2.5.1 Cylinder test

Forelimb use of the 32 rats was accessed after videotaping each rat for 10 min before AAV1/2 injection and 2, 4 and 6 weeks after injection. The rats were placed in a

transparent cylinder glass (diameter 20cm, height 30cm) individually when they were being recorded (Figure 3A). Two mirrors were placed in an angle behind the cylinder to allow the examiner to observe the rats clearly when they turned away from the camera. The videos were analyzed post-hoc by the experimenter blinded to the treatment conditions according to the statements from Schallert et al, 2000. The behaviors were analyzed for rearing movements along the wall and landing movements on the ground after a rear with either the ipsilateral paw or the contralateral paw or both paws simultaneously. Finally, the preference of the paw use was presented as percentage of the ipsilateral paw use with the equation: $(\text{ipsilateral paw} + 0.5 \text{ both paws}) / (\text{ipsilateral paw} + \text{contralateral paw} + \text{both paws}) \times 100\%$.

2.5.2 Pellet-reaching task

Motor performances of the contralateral paw of 24 rats were examined by pellet-reaching task. Rats were put in a Plexiglas box (34 cm x 14 cm) on each side, and they were trained to grasp one pellet from one side and pass it to the mouth, and then run to another side to grasp another pellet to eat (Figure 3B). After defining the paw preference of each rat, rats were trained to run back and forth and grasp pellets for 10 min every day. The training sessions took 19 days per rat. After all the rats were well trained, tests were performed and video-recorded before operation, and respectively 2, 4 and 6 weeks after operation. The success rate of the first 20 grasping attempts was analyzed for each rat. The scoring rules were as following: a score of 1 was given when rats successfully grasped the pellet and put it into the mouth, a score of 0.5 was given when rats got the pellet with paw however dropped it before eating, and a score of 0 was given when rats failed to get the pellet. Rats were trained every 5 days after OP, in order to maintain reproducibility. Four animals were excluded from the study for the reason that they were either uncooperative or the SN of these 4 rats were not successfully hit.

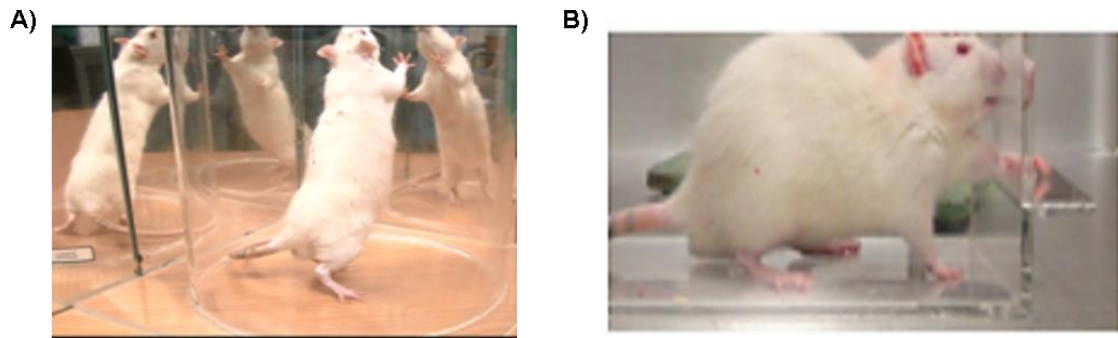


Figure 3: Images showing rat movements in behavioral tests.

A) Cylinder test: showing a rat rearing along the wall.

B) Pellet-reaching task: showing a rat grasping a pellet from the opening hole of the Plexiglas box.

2.6 Stereotaxic injection of AAV1/2 serotype

2.6.1 Preparing solutions for injection

1 μl AAV1/2-empty vector (EV) or 1 μl AAV1/2-A53T-aSyn viral vector designed as described by Koprach et al. (Koprach et al., 2010). 1 μl vector was dissolved in 5 μl Sterile 1 x phosphate buffered saline (PBS) so that at last the AAV1/2 was used at a concentration of 5.16×10^{12} genomic particles (gp)/ml. in normal Saline to a final concentration of 5mg/mg per kg of body weight (BW), injected 10 $\mu\text{l/g}$ BW s.c.. Both viral vector and Rimadyl were stored on normal ice.

2.6.2 AAV1/2 injection

Rimadyl medication was applied subcutaneously at least 30 minutes before surgery. Rats were supplied with isoflurane at a concentration of 3.5% and oxygen at a speed of 2L/min in an anesthesia box until they were deeply anesthetized. The effect of anesthesia was confirmed when defensive reflexes were abolished. Then rats were moved onto a stereotaxic frame with heating template placed below them, in order to administer and maintain body temperature at $37 \pm 0.5^\circ\text{C}$ (Figure 4). Afterwards isoflurane concentration was adjusted to a degree below 3.5% depending on the breathing speed and depth of the rats. After fixing the ear bars in both sides of the ears and fitting the rat mouse with the anesthesia mask, vet ointment was applied to the

eyes of the rats to avoid dryness under anesthesia conditions. A midline incision was made from between the rat eyes and extending 2 cm towards the posterior direction. Coordinates of bregma were determined after the coronal and sagittal sutures were clearly exposed. Afterwards, SN on either left or right side was orientated according to the Rat Brain Stereotaxic Coordinates of Paxinos and Watson (Paxinos and Watson, The Mouse Brain in Stereotaxic Coordinates, Sixth Edition, 2001). The coordinates of SN from Bregma are: AP -5.1mm; ML: ± 2 mm; DV: -7.4mm. Injections were applied with the microinjection syringe (Hamilton Co., Reno, NV, USA). Incisions were closed after injection and alcohol was applied to the surface of the incision. Then rats were transferred to a heater keeping the temperature at 37°C until they woke up. 36 rats were injected with AAV1/2-A53T-aSyn, and another 33 rats were injected with AAV1/2-EV. 6 animals were excluded from the study because of unsuccessful injections into SN.

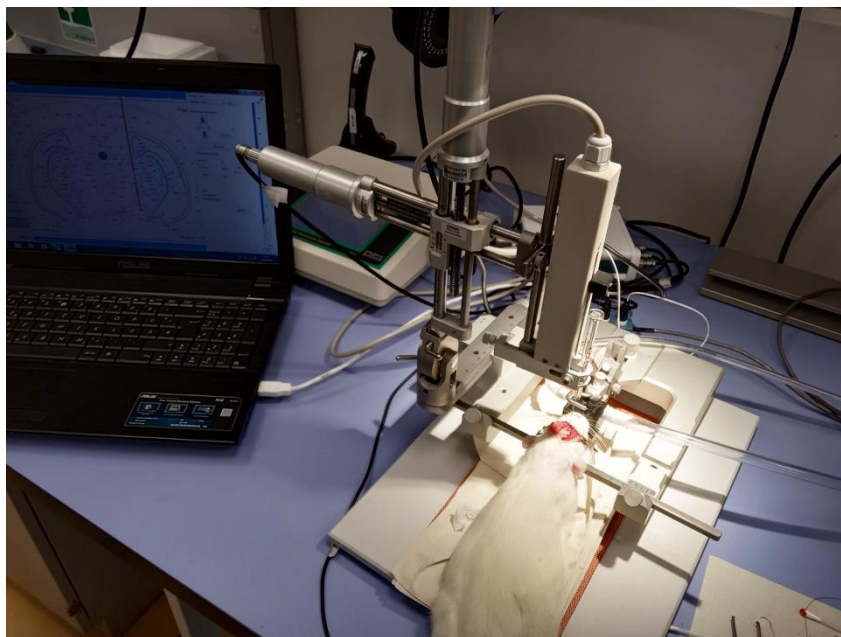


Figure 4: Stereotaxic injection in rat brain.

2.7 Tissue processing

2.7.1 Horizontal 10° fresh frozen sections

Rats were euthanized 2, 4 and 6 weeks respectively after disease induction by exposure to CO₂. Afterwards each rat was transcardially perfused with 60 ml heparinized 0.1M PBS. Rat brains were carefully extracted from the brain skull and then washed with PBS.

Then, rat brains were placed horizontally in a cryomold filled with OCT medium (Sakura, Germany) and were immediately frozen in liquid dry ice-cooled methylbutane. Frozen brains were stored at -20° . At last, brains were cryo-sliced into $10\ \mu\text{m}$ sections with an angle of 10° and mounted on object slides (2 sections on one slide). Altogether 36 rats were cut into horizontal 10° sections which have been used for analyzing molecules associated with neurodegeneration, TH + DA neurons and TH optical density in the nigrostriatal tract.

2.7.2 Coronal free-floating sections

Rats were perfused the same way as for horizontal 10° sections. Next, rat brains were placed in a brain matrix slicer and were dissected coronally at -0.26mm from bregma (Figure 18, Paxinos and Chales Watson, rat brain atlas). The dorsal part of the dissected brain, including the SN, was immersion-fixed in 4% paraformaldehyde (PFA) in 0.1 M of PBS for 2 days at $4\ ^{\circ}\text{C}$. And then the brains were transferred to 30% sucrose in 0.1M of PBS solution and stored at $4\ ^{\circ}\text{C}$ for another 4 days. After dehydration, brains were frozen in OCT medium (Sakura, Germany) cooled by dry ice. At last, rat brains were cryo-sectioned into $40\ \mu\text{m}$ per section in 6 series and preserved in an anti-freeze cryoprotectant at -20°C . In total 27 rats were cut into coronal sections and used for counting of dopaminergic neurons in SN.

2.8 Immunohistochemistry

2.8.1 Tyrosine hydroxylase (TH) staining

Tyrosine hydroxylase staining was used to mark the nigrostriatal tract in $10\ \mu\text{m}$ horizontal 10° rat brain sections. First of all, sections were circled with liquid blocker and then post-fixed with 4% PFA for 15 min at room temperature (RT) followed by section washing for 3×5 min. Blocking was performed for 1h at RT with 2% normal bovine serum (BSA) and 10% normal goat serum (NGS) in 0.01 M PBS. After that sections were incubated overnight at RT with rabbit anti-rat TH primary antibody (Abcam, UK) diluted in 2% BSA and 2% NGS in 0.01 M PBS. Sections were again carefully washed for 3×5 min. And then secondary biotinylated goat anti-rabbit antibody (Vector Laboratories cat, USA) was applied to the sections for 1 hour at RT, followed by another 3×5 min wash.

Moreover, incubation of Ultra-sensitive avidin/biotin complex (ABC) was performed. At last, diaminobenzidine (DAB)-Peroxidase substrate solution (Vector Labs, USA) incubation was applied until the staining was visualized. Sections were then covered with aqueous mounting media (Darmstadt, Germany). In addition, control stainings without the primary antibody or the secondary antibody were performed.

2.8.2 TH/Nissl staining

One series of the rat sections was randomly selected for TH staining of the 40 μm coronal free-floating sections, to label TH + dopaminergic neurons in SN. Sections were washed with distilled water for 5 min before incubating with blocking solution followed by incubation of primary antibody overnight at 4°, secondary antibody for 2 hours at RT, avidin/biotin solution for 2 hours at RT and at last DAB - Peroxidase substrate solution at RT. All the above incubations were performed on a shaker except for the DAB-Peroxidase substrate solution. All the antibodies and solutions for TH stainings of the 40 μm coronal free-floating sections are the same as shown above for TH staining in the 10 μm horizontal 10° section. Sections were dried for around 1 hour at RT after TH staining and then put into cresyl-violet solution for 30 min at RT. After washing in distilled water, sections were dehydrated in an ascending ethanol series: 70% Ethanol (EtOH) for 3 \times 1min, 96% EtOH for 2 \times 1min, 100% EtOH for 1min and then in 100% EtOH for 35s. At last, sections were incubated in xylene solution (St. Louis, USA) for 2 \times 5 min and covered with slips. In addition, control stainings without the primary antibody or the secondary antibody were performed.

2.8.3 TH/aSyn immunofluorescence double staining

Sections were first circled with Pap pen (Science Services, Germany) and post-fixed with 4% PFA for 15 min at RT followed by washing for 3 \times 5 min with 1 \times PBS. Blocking solution composed of 5% BSA and 5% NGS in 0.1 M PBS was applied to the rat sections. After washing for 3 \times 5 min sections were incubated with primary chicken-anti-rat TH (Abcam, UK) and mouse-anti-human aSyn (Invitrogen, USA) antibodies overnight at 4°. After another 3 \times 5 min wash sections were incubated with fluorescence-labeled goat-anti-chicken Cy3 (Alpha Diagnostics, USA) and goat-anti-mouse Cy2 (Jackson ImmunoResearch Laboratories Inc., PA) secondary antibodies for 1h followed by PBS

wash for 3× 5 min. Lastly, 4',6-diamidino-2-phenylindole (DAPI) nuclear staining (Sigma-Aldrich, USA) was performed at RT for 20 minutes. All sections were covered with Aqua Polymount (Warrington, PA). In addition, control stainings without the primary antibody or the secondary antibody were performed.

2.8.4 Immunofluorescence double staining of TH and pro- and antidegeneration markers

The staining process and all the solutions and antibodies are the same as used for TH/aSyn immunofluorescence double staining shown above except for the primary antibodies used for pro- and antidegeneration molecules: rabbit-anti-rat Nrf2 (GeneTex, USA), rabbit-anti-rat Tau (Sigma, USA) and rabbit-anti-rat NMNAT2 (Biorbyt, UK) and rabbit-anti-rat SARM1 (MyBioSource, USA). The secondary antibody used for all these 5 molecules is goat-anti-rabbit alexa fluor 488 (Invitrogen, USA). In addition, control stainings without the primary antibody or without the secondary antibody were performed. No specific signal of the pro- and antidegeneration molecules in the control stainings was observed. In addition, control stainings without the primary antibody or the secondary antibody were performed.

2.9 Unbiased stereology for SN neurons

Stereology was performed on the rat coronal sections to count the number of TH+ dopaminergic neurons in SN with the help of the Stereo Investigator software package 11.07 (MicroBrightField Biosciences, VT). The analyst was blinded to the treatment conditions of all the rats by coding the object slides. In average, a series of 12 sections (1/6 series) of one rat separated by 240 μm were used for counting after TH immunohistochemical staining. TH+ neurons and Nissl+ neurons in SN pars compacta and reticulata were included within the selected region for quantification. Parameters for counting were as follows: grid size 130 × 130 μm , counting frame 60 × 60 μm , and guard zone 1.5 μm . Actual mounted thickness was determined by randomly selecting sections and determining thickness at every counting site. Sections were viewed under a 1003/1.25 numerical aperture objective (Olympus, Japan) on a BX53 microscope

(Olympus, Japan). Gundersen coefficients of error should be less than or equal to 0.09 for each section counted.

2.10 Image processing

2.10.1 Optical density analysis of TH+ dopaminergic axons and TH+ dopaminergic fibers in the striatum

Optical density of the TH+ dopaminergic axons and fibers in the striatum on horizontal 10° sections were analyzed by NIH ImageJ software (LOCI, University of Wisconsin). Images were firstly transformed into 8-bit greyscale and then inversed in order to make the stained structures more visible. Corpus callosum with weak staining was used to determine the staining background and both sides of the sections were subtracted with the background intensity. Finally, the intensity of the dopaminergic axons and fibers in the striatum was measured and the values were normalized by dividing injected side with uninjected side of the section (animal number $n \geq 6$ in A53T-aSyn groups and A53T-EV groups at 2w, 4w and 6w time point). No specific signal of TH in the control stainings was observed.

2.10.2 Cell counting of TH+ and Nissl+ DA neurons

TH+ DA neurons within SN pars compacta and reticulata were counted on the horizontal 10° sections. The neuron number of the injected side were standardized by the number of the uninjected side of the sections (animal number $n \geq 4$ in A53T-aSyn groups and A53T-EV groups at 2w, 4w and 6w time point). No specific signal of TH or Nissl in the control stainings was observed.

2.10.3 Immunofluorescence intensity analysis of pro- and antidegeneration markers

Immunofluorescence images of pro- and antidegeneration markers were first transformed into 16-bit greyscale using ImageJ and then black and white inverted to enhance the contrast of the stained structures to mark the region of interest. Next, background intensity for each position in the proximity of selected region of interest in the extracellular tissue was subtracted. And then, the areas of stainings for pro- and

antidegeneration markers which are TH-immunoreactive on the TH staining images were circled and the intensity was measured. In SN, ten dopaminergic perikarya on the staining images of the pro- and antidegeneration molecules which are colocalized with the DA neurons on the TH staining images were chosen to get the average value. Areas of TH-immunoreactive axon bundles on the staining images of the pro- and antidegeneration molecules were chosen. In STR, 5 areas which are not localized in the TH-positive cell bodies in the STR are chosen as terminals. Lastly, the values of intensity were normalized by dividing injected side with uninjected side of the section ($n \geq 6$ in A53T-aSyn groups and A53T-EV groups at 2w, 4w and 6w time point). No specific signal of the pro- and antidegeneration molecules in the control stainings was observed.

2.11 Statistical analysis

Before performing statistical analysis, normal distribution was confirmed by Shapiro-Wilk normality test using Graphpad Prism 7 software (San Diego, USA). For the cylinder test, pellet-reaching task, analysis of TH+ optical density in axons and striatum, TH+ DA numbers in SN, immunofluorescence intensity analysis of Nrf2, in SN and axons, intensity analysis of NMNAT2 in SN, the parametric one-way analysis of variance (ANOVA) test with Turkey's multiple comparison post-test was performed. In case of non-normal distributed data for immunofluorescence intensity analysis of Nrf2 in striatum, NMNAT2 in axons and striatum, Sarm1 in SN, striatum and axons, non-parametric Kruskal-Wallis test followed by Mann-Whitney test was implemented. Correlations were calculated using Pearson r followed by a subsequent linear regression analysis. * $p < 0.05$, ** $p < 0.01$, *** $p < 0.001$ and **** $p < 0.0001$ were considered as significant P-values.

3 Results

3.1 The nigrostriatal tract is best visible in horizontal 10° sections

The nigrostriatal tract can be traced from dopaminergic cell bodies in SN through dopaminergic axons to the dopaminergic terminals in striatum in horizontal 10° sections (Figure 5)

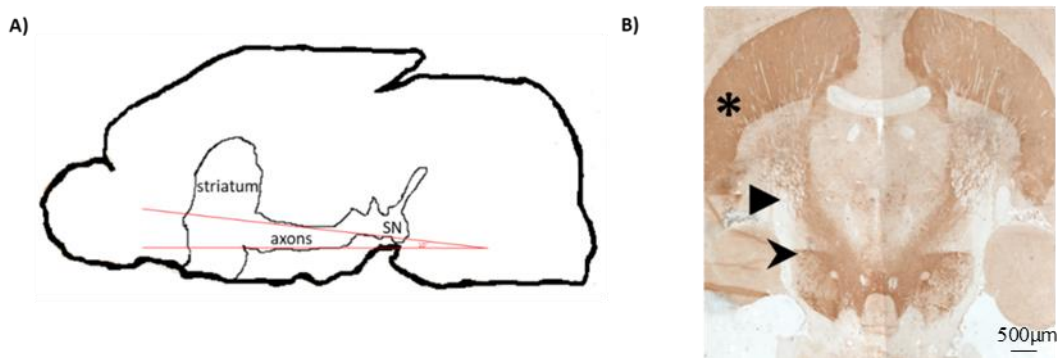
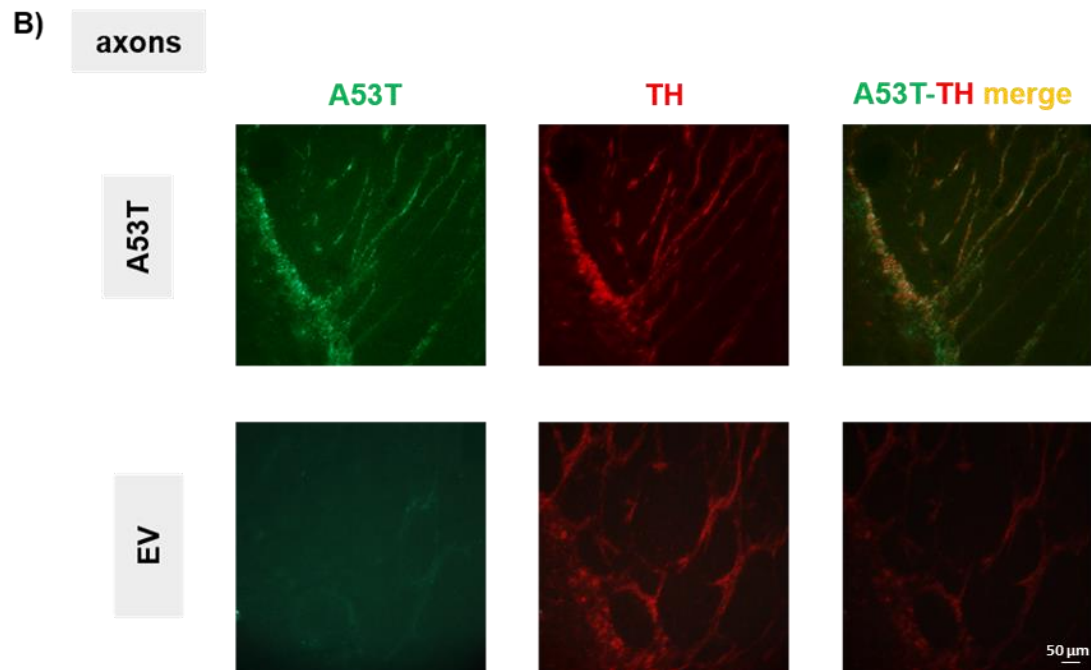
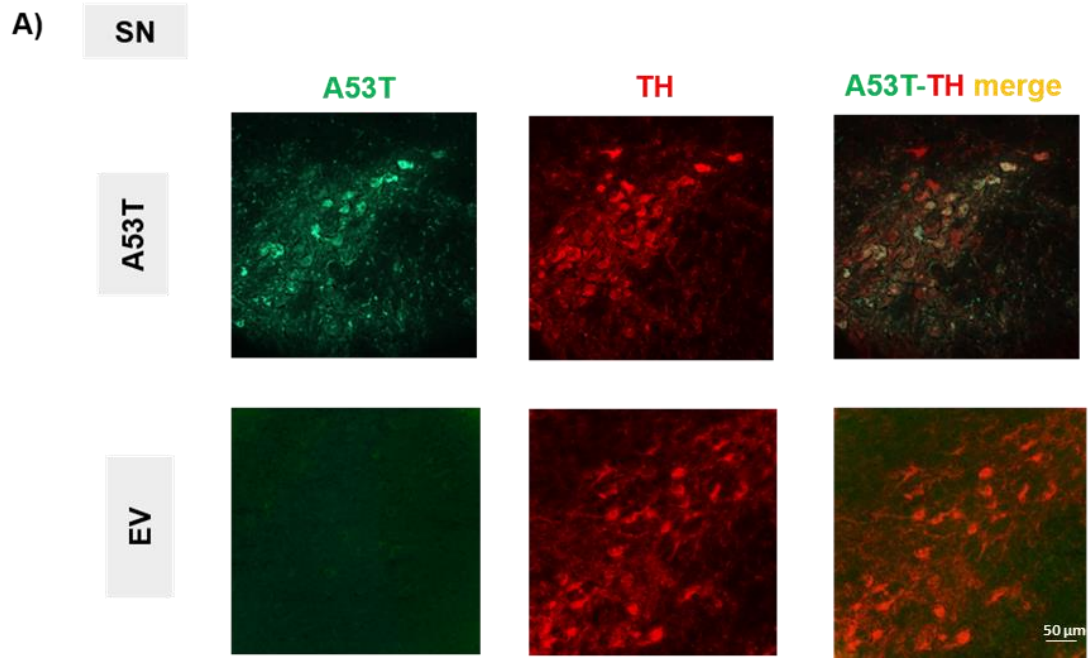


Figure 5: Immunohistochemical staining for TH as marker of the dopaminergic tract.

A) The cutting angle of horizontal 10° shown in sagittal scheme. B) The dopaminergic neurons in the substantia nigra (triangular arrowhead), dopaminergic axons (arrow) and the dopaminergic terminals in the striatum (asterisk) could be clearly visualized.

3.2 Verification of AAV1/2-A53T-aSyn injection in the rat SN

Homogenous and widespread spread AAV1/2-A53T-aSyn along the whole dopaminergic tract verifies successful injection of AAV1/2-A53T-aSyn into SN (Figure 6).



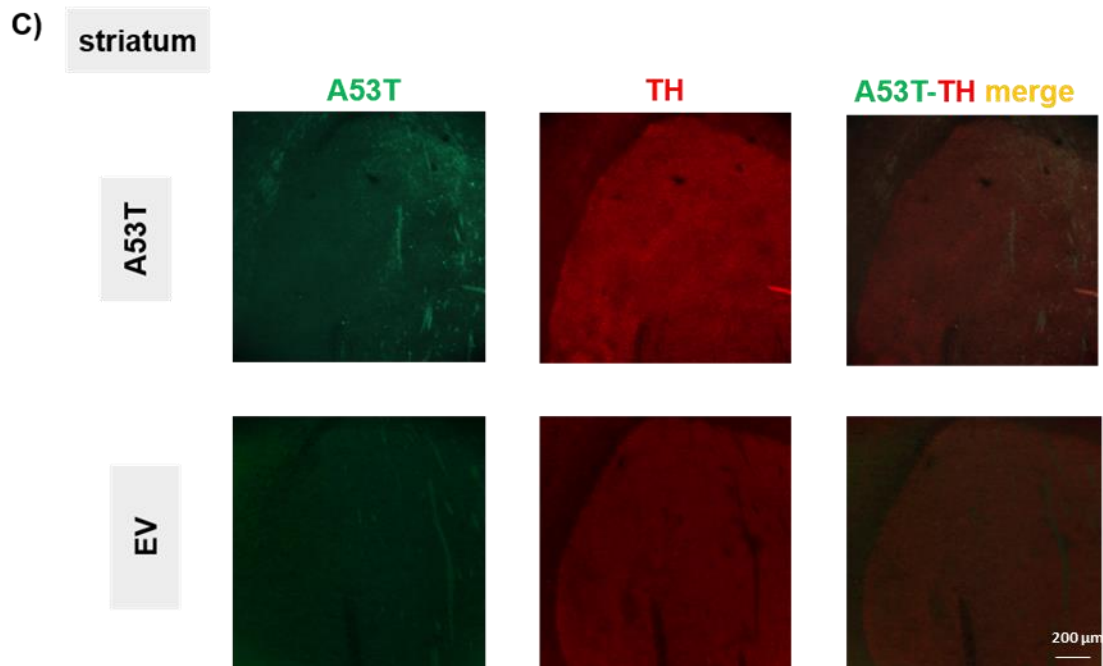


Figure 6: Immunofluorescence double stainings of human aSyn (green) and TH (red).

AAV1/2-induced A53T-aSyn is transported from A) SN through B) dopaminergic axons to C) striatum. Note: A53T stands for AAV1/2-induced A53T-aSyn, EV stands for AAV1/2-induced empty vector.

3.3 Time-dependent progressive motor impairment of the contralateral paw in the AAV1/2-A53T-aSyn PD rat model

In cylinder test, progressive motor impairment of the contralateral paw in A53T-aSyn rat groups developed starting from 2 weeks after viral vector injection. At 4 weeks ($p < 0.0001$) and 6 weeks ($p < 0.001$) after disease induction, significant paw asymmetry of the A53T-aSyn rat groups was observed comparing to EV groups at the same time points (Figure 7A).

Similar as the case in cylinder test, slight motor deficit of the contralateral paw displayed 2 weeks post injection in pellet reaching task. At 4 weeks ($p < 0.05$) and 6 weeks ($p < 0.05$) post injection, significant motor dysfunction of the A53T-aSyn rats developed as compared to EV groups at the respective time points (Figure 7B, 7C).

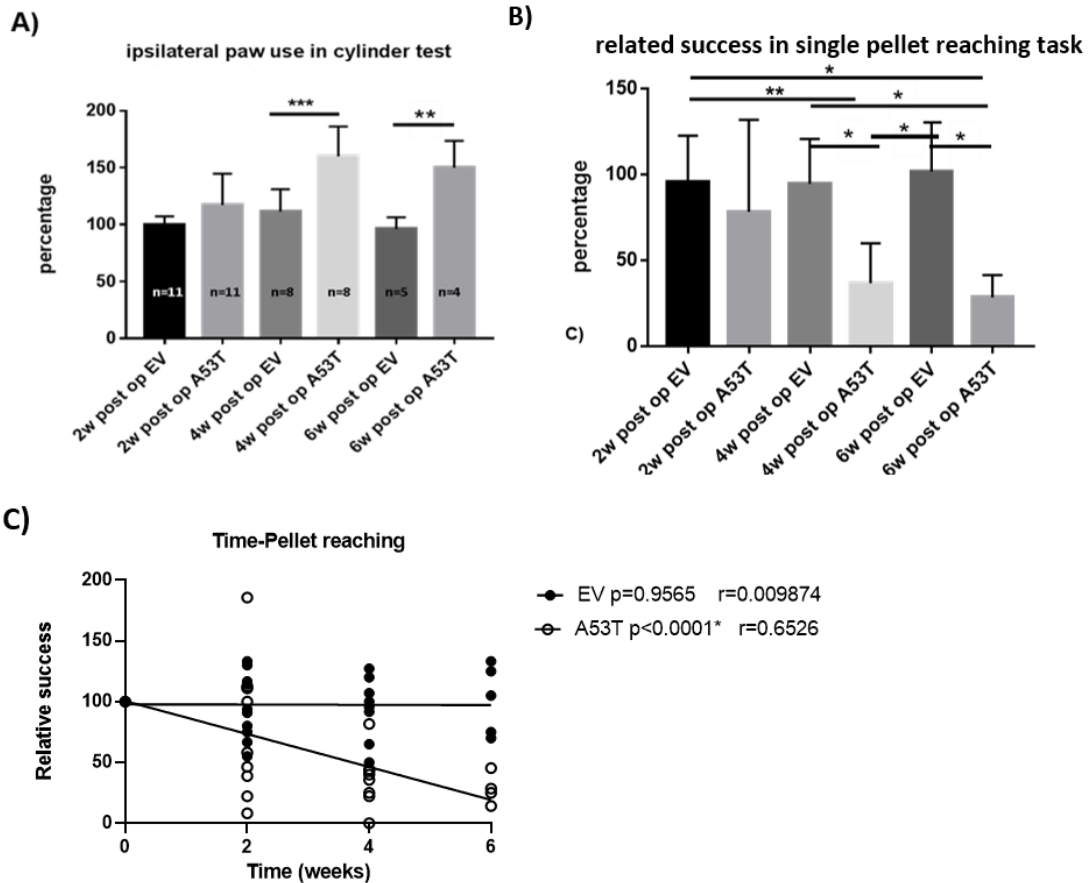
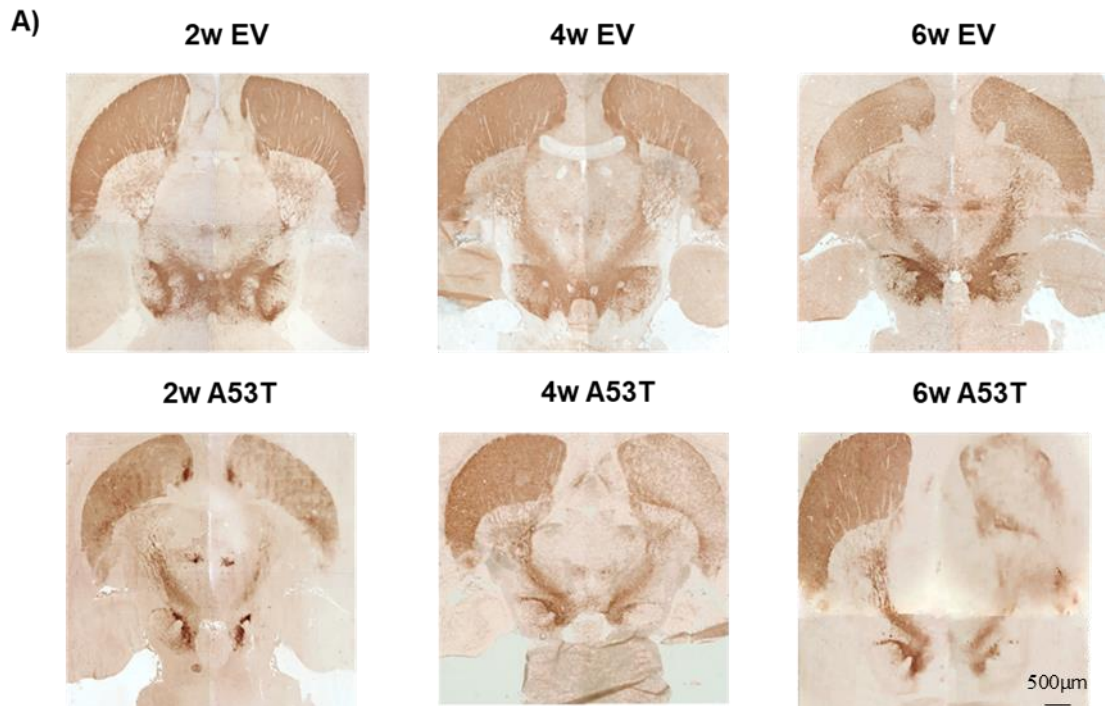


Figure 7: Results of behavioral tests of EV and A53T-aSyn rat groups respectively 2 weeks, 4 weeks and 6 weeks after injection.

A) Percentage of the ipsilateral paw use of all rat groups at 2 weeks, 4 weeks and 6 weeks to pre-op paw use in cylinder test. Slight difference was shown between EV groups and A53T-aSyn groups 2 weeks post injection, however at 4 weeks ($p<0.001$) and 6 weeks ($p<0.001$) after injection, use of the contralateral paw in the A53T-aSyn groups was significantly lower as compared with EV groups at respective time points. B) Percentage of related success of all rat groups at 2 weeks, 4 weeks and 6 weeks divided by pre-op values in single pellet reaching task. No significant difference was detected between EV group and A53T group after 2 weeks, whereas success rate of the A53T-aSyn rat groups were significantly lower as compared to EV groups at 4 weeks ($p<0.05$) and 6 weeks after injection ($p<0.05$). C) Correlation analysis with simple linear regression reveals time-dependent progressive behavioral changes in A53T-aSyn rats. * $p<0.05$, ** $p<0.01$, *** $p<0.001$.

3.4 Time-dependent progressive neurodegeneration of nigrostriatal dopaminergic tract in the AAV1/2-A53T-aSyn PD rat model

Time-dependent progressive degeneration of the dopaminergic tract in the A53T-aSyn groups started from 2 weeks time point. At 4 weeks time point, significant degeneration of dopaminergic neurons in the SN ($p < 0.05$) developed in the A53T-aSyn groups. At 6 weeks, substantial degeneration of both dopaminergic fibers in the striatum ($p < 0.01$) and dopaminergic neurons ($p < 0.01$) in the SN could be observed. However, a slight but nonsignificant degeneration of dopaminergic axons was found at all the three time points (Figure 8).



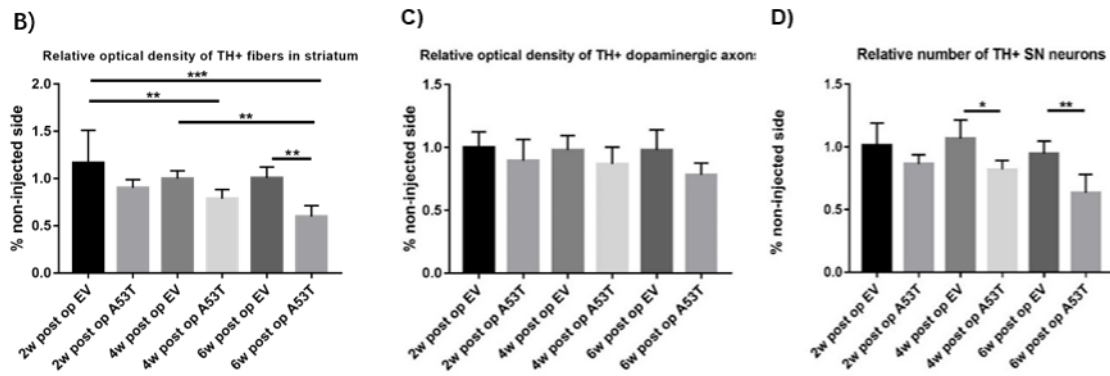


Figure 8: Relative optical density or relative cell number in the TH+ dopaminergic tract of EV and A53T-aSyn rat groups respectively 2 weeks, 4 weeks and 6 weeks after injection.

A) Immunohistochemical stainings of TH for nigrostriatal dopaminergic tract in the horizontal 10° sections of EV and A53T-aSyn rat groups respectively 2 weeks, 4 weeks and 6 weeks after injection. B) Relative optical density of TH+ fibers in the striatum in the injected side divided by the uninjected side. A continuous decline of TH+ fiber density starting from 2 weeks was shown. At both 2 weeks and 4 weeks time points, no substantial decline was investigated between EV and A53T-aSyn groups. However, 6 weeks after disease induction, significant reduction of the relative optical density of TH+ fibers in striatum was observed in the A53T-aSyn groups as compared to EV groups ($p < 0.01$). C) Relative optical density of TH+ axons in the injected side divided by the uninjected side. A continuous decline of TH+ axon density starting from 2 weeks post op was shown. However no significant reductions of axon density were observed between EV and A53T-aSyn groups at all time points. D) Relative TH+ number in the SN in the injected side divided by the uninjected side. A continuous decrease of TH+ number in the SN starting from 2 weeks. At 4 weeks and 6 weeks, substantial decline of TH+ DA neurons in the A53T-aSyn rat groups was found comparing to respectively 4w EV group and 6w EV group. * $p < 0.05$, ** $p < 0.01$.

3.5 Time-dependent progressive loss of TH/Nissl+ SN neurons in the AAV1/2-A53T-aSyn PD rat model

Time-dependent loss of TH+ dopaminergic neurons in PD rats started 2 weeks after disease induction, whereas significant time-dependent loss of Nissl+ SN neurons was found starting 4 weeks after disease induction (Figure 9).

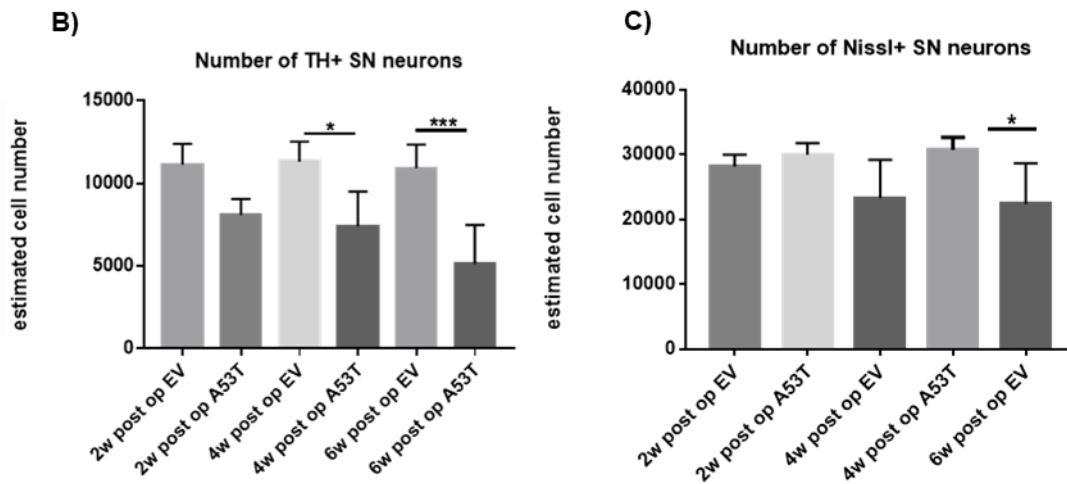
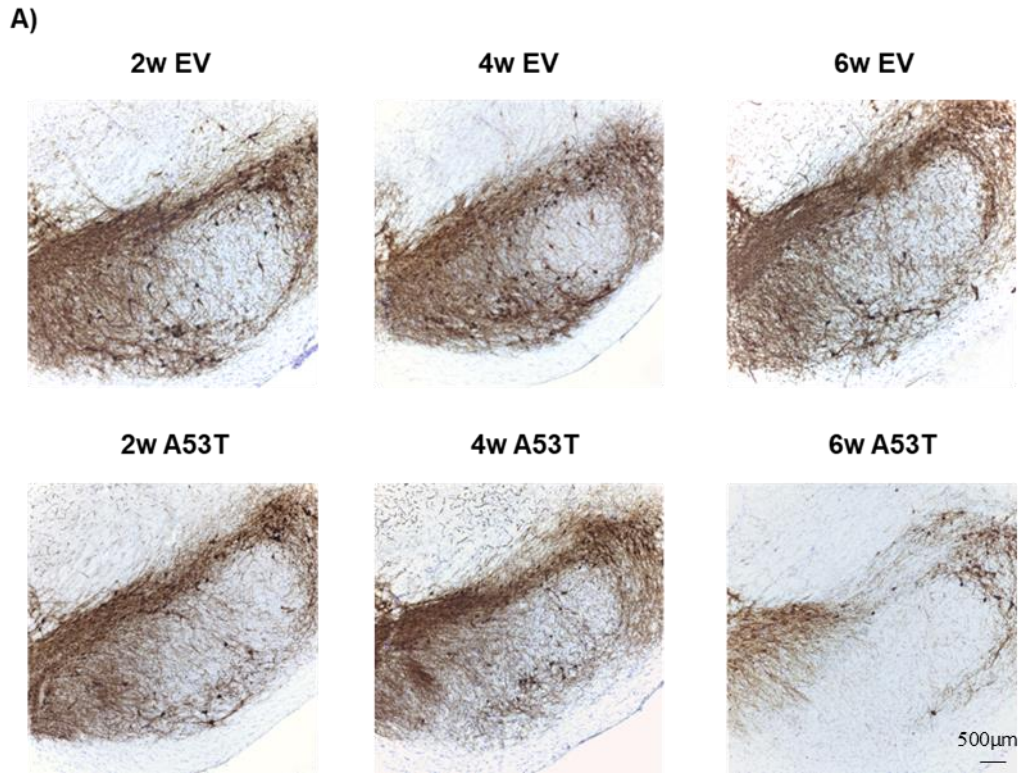


Figure 9: TH stainings and estimated cell number of TH+ SN neurons in EV and A53T-aSyn rat groups respectively 2 weeks, 4 weeks and 6 weeks after injection.

A) Immunohistochemical TH stainings in the SN for rat groups of EV and A53T groups at 2 weeks, 4 weeks and 6 weeks time points. B) Stereologically estimated cell number of TH+ SN neurons. At 4 weeks ($p < 0.01$) and 6 weeks ($p < 0.001$), a substantial decrease of TH+ neurons was detected comparing EV groups and A53T-aSyn groups at respective time points. C) Estimated cell number of Nissl+ SN neurons. At 6 weeks time point, reductions of Nissl+ SN

neurons was observed comparing 6w EV group ($p < 0.05$) with 6w A53T-aSyn group. * $p < 0.05$, ** $p < 0.01$, *** $p < 0.001$, **** $p < 0.0001$.

3.6 Progressive motor deficits correlate with striatal dopaminergic denervation but not with dopaminergic perikarya loss in the AAV1/2-A53T-aSyn PD rat model

Motor deficit in relative single pellet reaching task does not correlate to the relative number of TH+ neurons in SN at six weeks' time point. However, it correlates to the degeneration of dopaminergic terminals in the striatum at six weeks' time point (Figure 10).

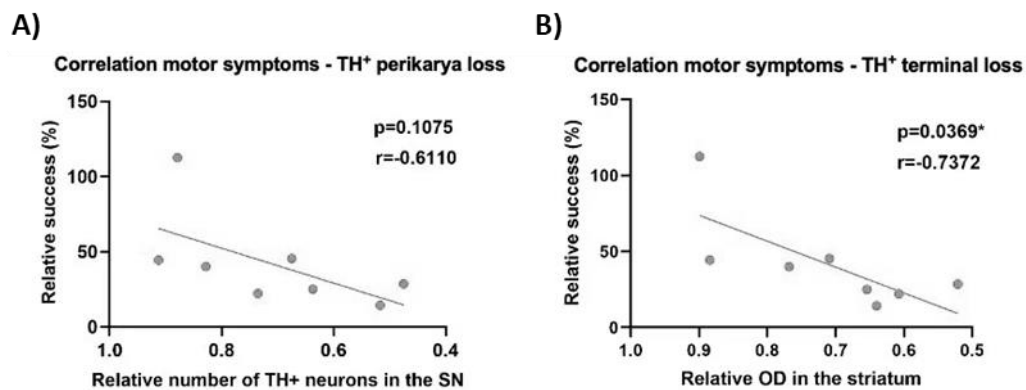
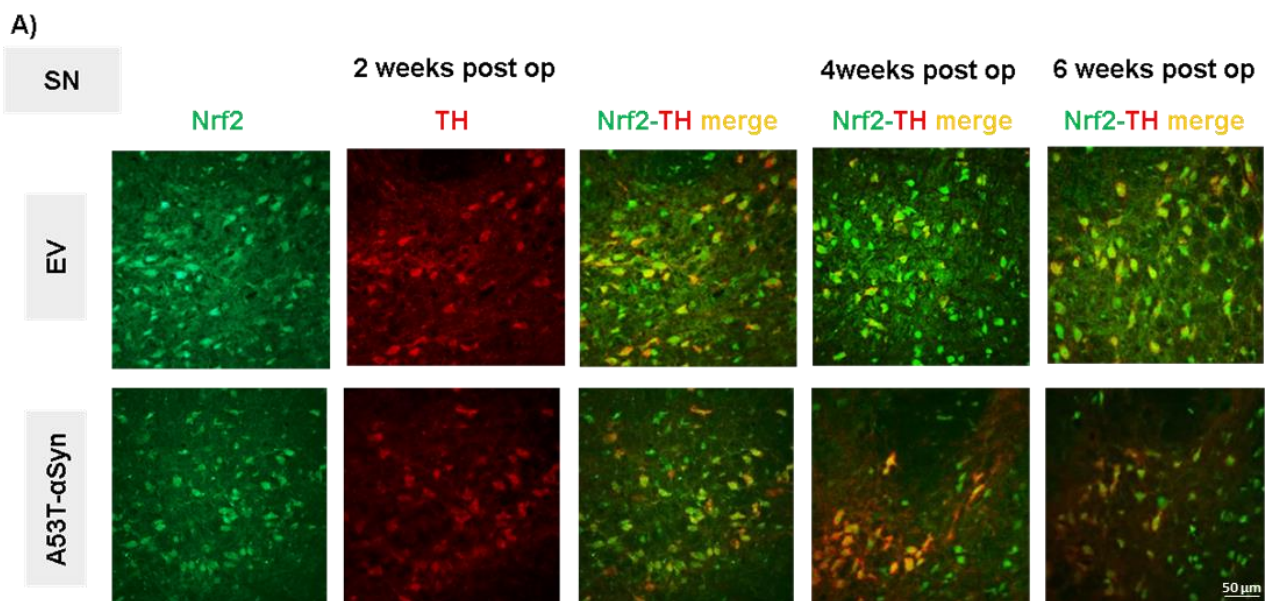


Figure 10: Motor deficits in A53T-aSyn PD rats correlate with dopaminergic terminal loss in the striatum

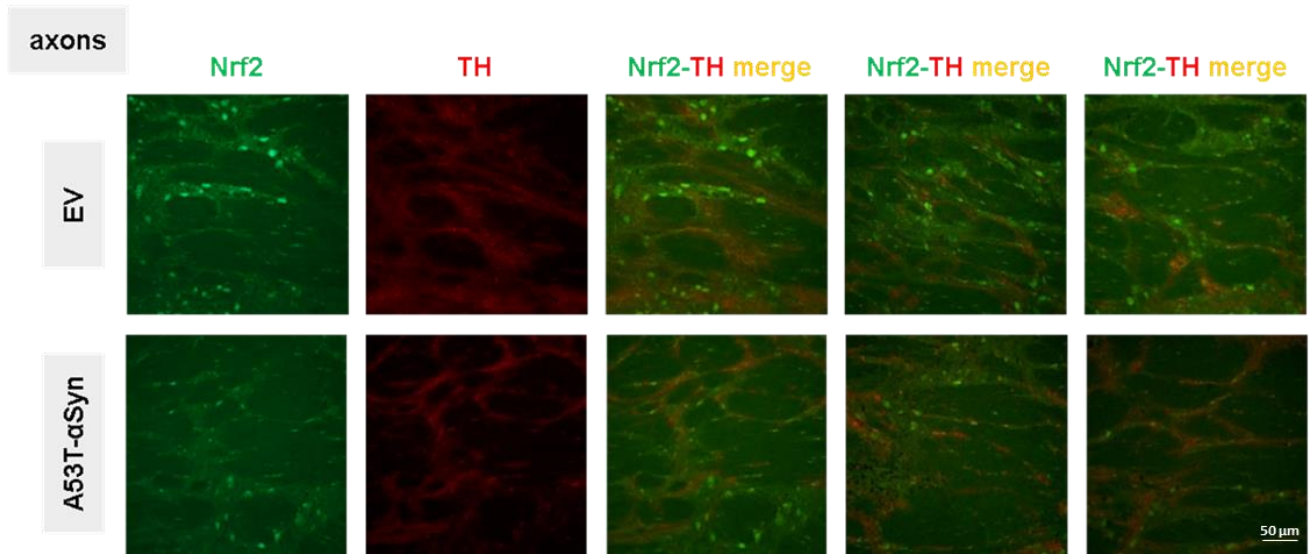
A) Decline of motor performance in relative single pellet reaching task does not correlate to the relative number of TH+ neurons in the substantia nigra at six weeks' time point but B) correlates significantly to the loss of dopaminergic terminals in the striatum at six weeks' time point using simple linear regression analysis. The A) $r = -0.6110$, $p = 0.1075$, B) $r = -0.7372$, $p = 0.0369^*$ (Correlation analyses were performed by Dr. T. Musacchio).

3.7 Downregulation of Nrf2 expression in the nigrostriatal perikarya and in the TH-immunoreactive axons of the AAV1/2-A53T-aSyn PD rat model

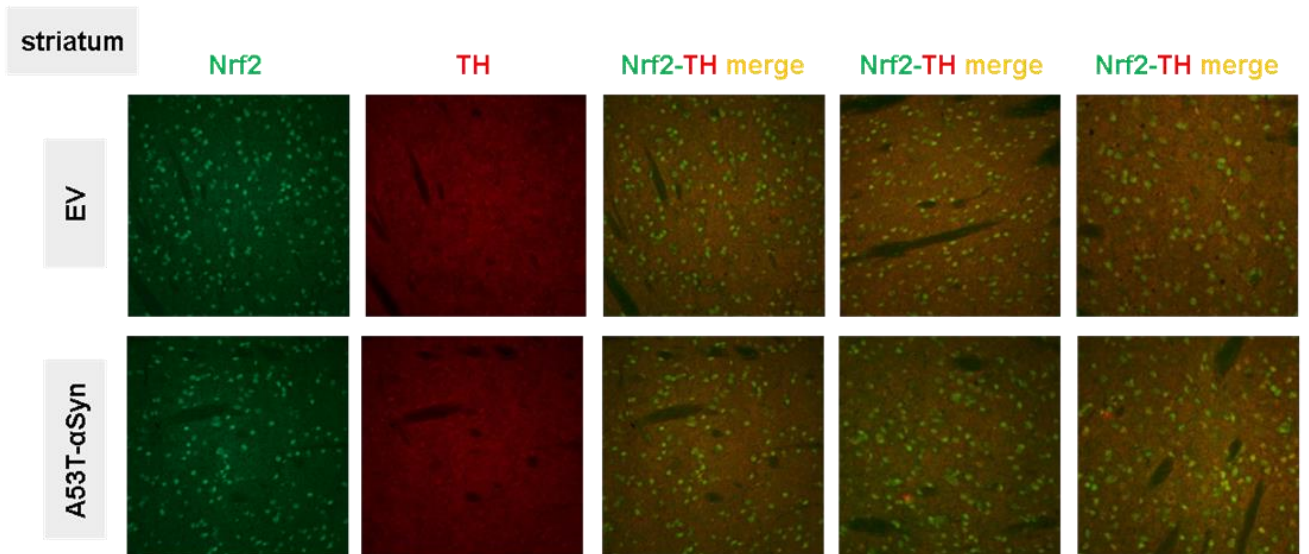
2 and 4 weeks after injection, slight but nonsignificant downregulations of Nrf2 expression were showed in the nigrostriatal perikarya and in the localization of the associated TH-immunoreactive axon bundles in A53T-aSyn groups compared to EV groups, whereas 6 weeks after injection substantial downregulations of Nrf2 in A53T-aSyn groups developed in nigrostriatal perikarya ($p < 0.05$) and TH-immunoreactive axons ($p < 0.05$). However in the striatum no significant alterations were found at all time points (Figure 11).



B)



C)



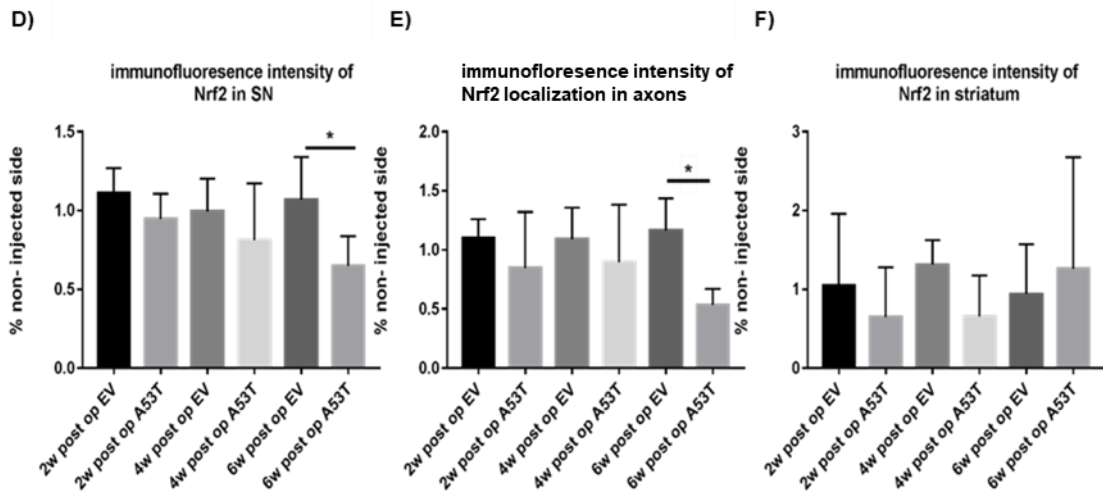
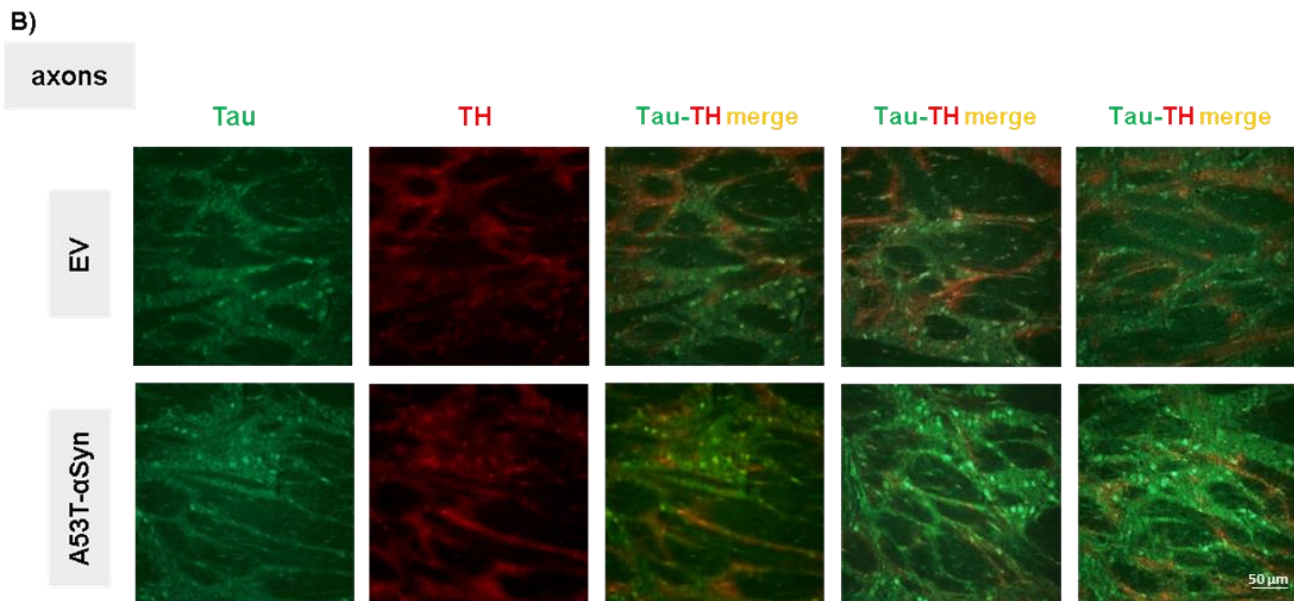
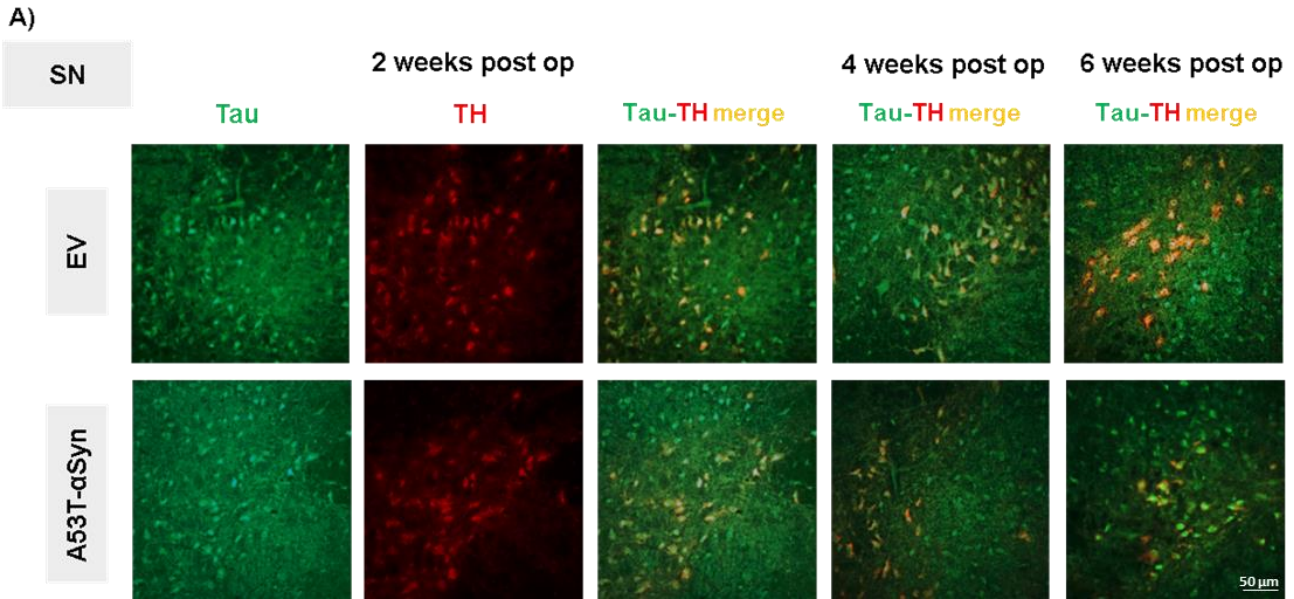


Figure 11: Immunofluorescence stainings and intensity analysis of Nrf2 expression in the dopaminergic nigrostriatal tract of EV and A53T-aSyn rat groups respectively 2 weeks, 4 weeks and 6 weeks after injection.

A, B, C) Immunofluorescence stainings of Nrf2 (green) and TH (red) of dopaminergic perikarya, TH-immunoreactive axons and striatal fibers of horizontal 10° rat sections 2, 4 and 6 weeks after injections, respectively. D, E, F) Immunofluorescence intensity analysis of Nrf2 stainings showed a trend of Nrf2 decline in both dopaminergic perikarya and TH-immunoreactive axons starting from 2 weeks after injections, and downregulation of Nrf2 in dopaminergic neurons and TH-immunoreactive axons in PD rats 6 weeks after disease induction was observed ($p < 0.05$). However in dopaminergic fibers in the striatum, no clear trend of alteration was observed at all time points. * $P < 0.05$.

3.8 A trend of nonsignificant Tau downregulation in the nigrostriatal perikarya and nonsignificant upregulation in the TH-immunoreactive axons of the AAV1/2-A53T-aSyn PD rat model

A trend of nonsignificant Tau downregulation in the nigrostriatal perikarya and nonsignificant upregulation in the TH-immunoreactive axons starting from 2 weeks after injection developed in the A53T-aSyn rat groups as compared to EV groups. However in the striatum no significant alterations were found at all time points (Figure 12).



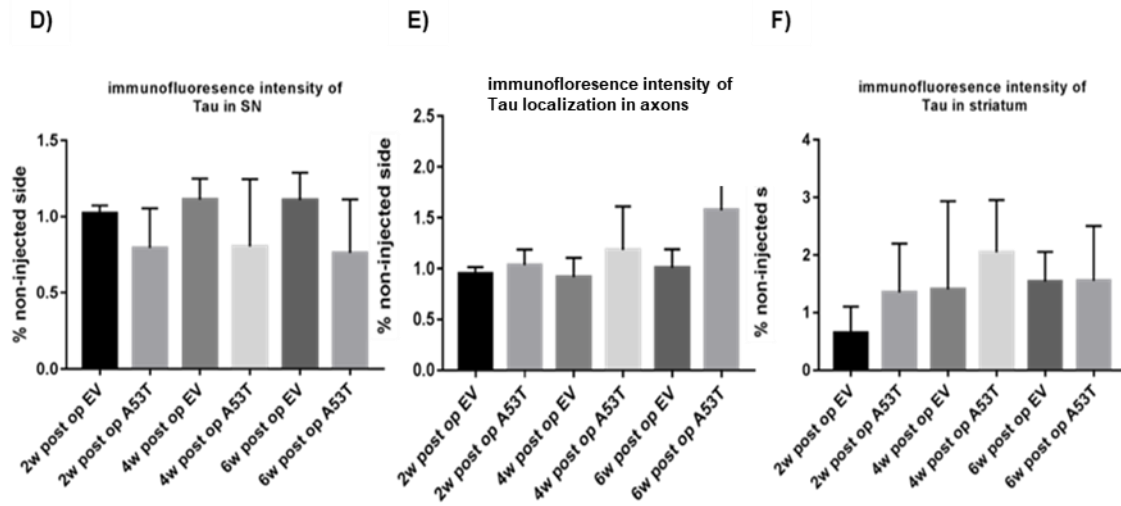
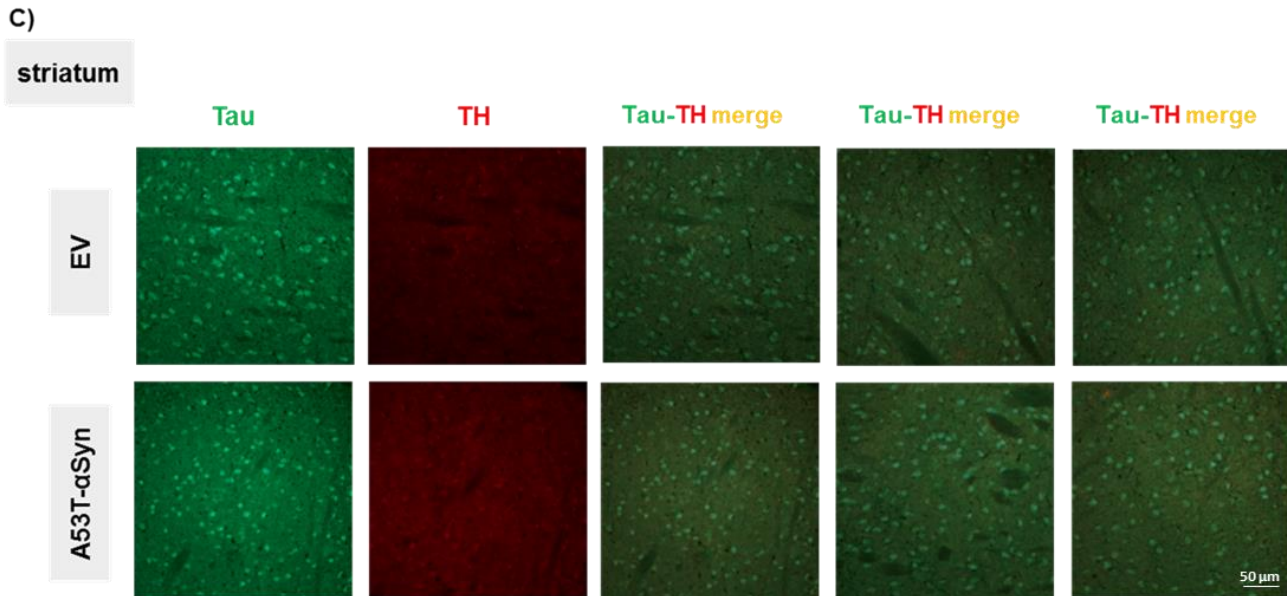
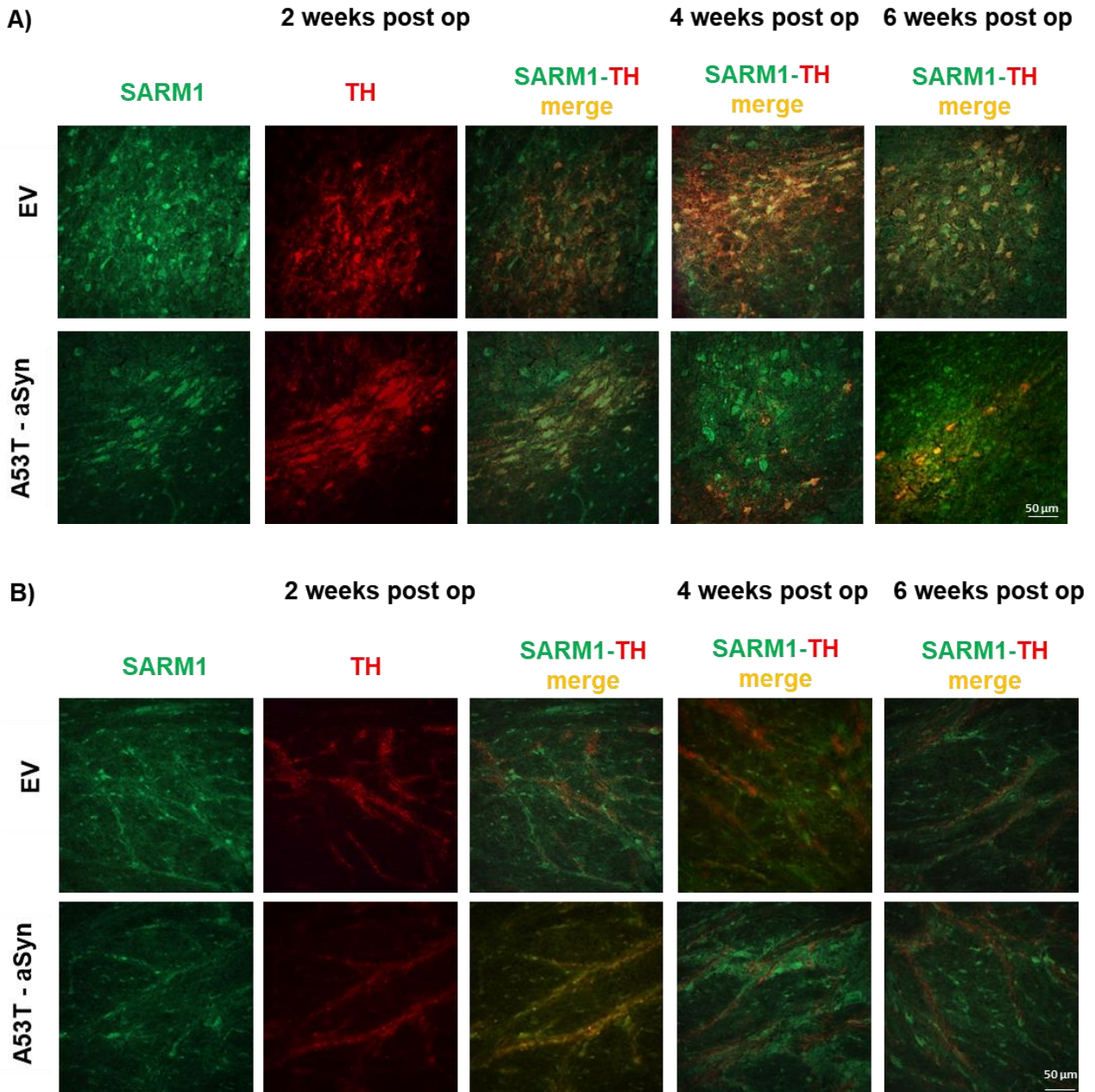


Figure 12: Immunofluorescence stainings and intensity analysis of Tau expression in the dopaminergic nigrostriatal tract of EV and A53T- α Syn rat groups respectively 2 weeks, 4 weeks and 6 weeks after injection.

A, B, C) Immunofluorescence stainings of Tau (green) and TH (red) of dopaminergic perikarya, axons and striatal fibers of horizontal 10° rat sections 2, 4 and 6 weeks after injections, respectively. D, E, F) Immunofluorescence intensity analysis of Tau stainings showed a nonsignificant decrease of Tau signal in dopaminergic perikarya and a nonsignificant increase of Tau signal in TH-immunoreactive axons starting from 2 weeks. However, in dopaminergic fibers in the striatum, no clear trend of alteration was observed at all time points.

3.9 No evident alterations of SARM1 expression in the nigrostriatal tract of the AAV1/2-A53T-aSyn PD rat model

No significant regulations of SARM1 in the nigrostriatal tract in A53T-aSyn rat groups displayed comparing with EV rat groups (Figure 13).



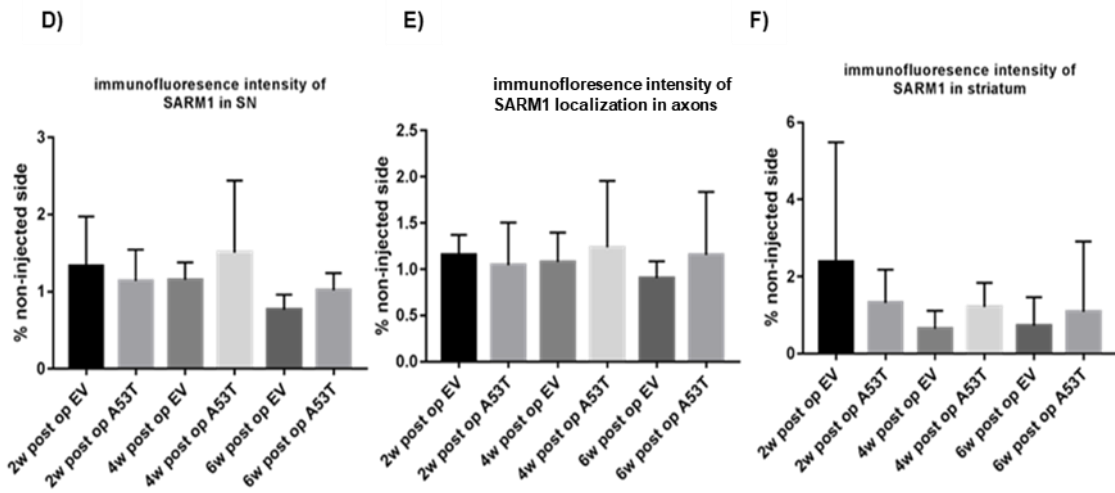
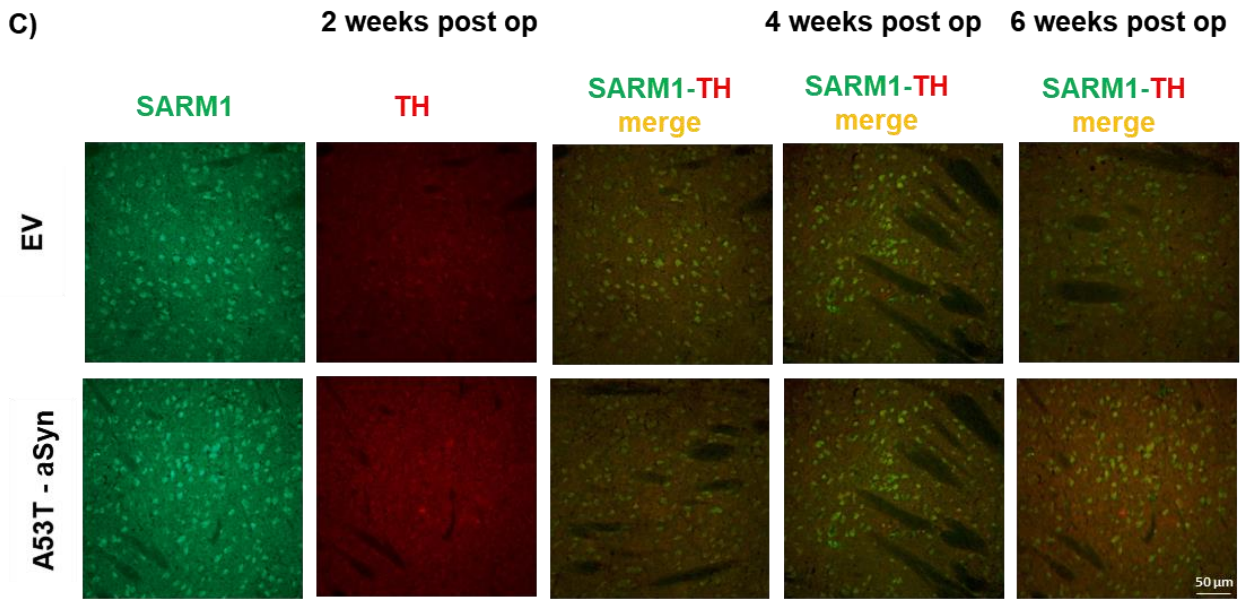
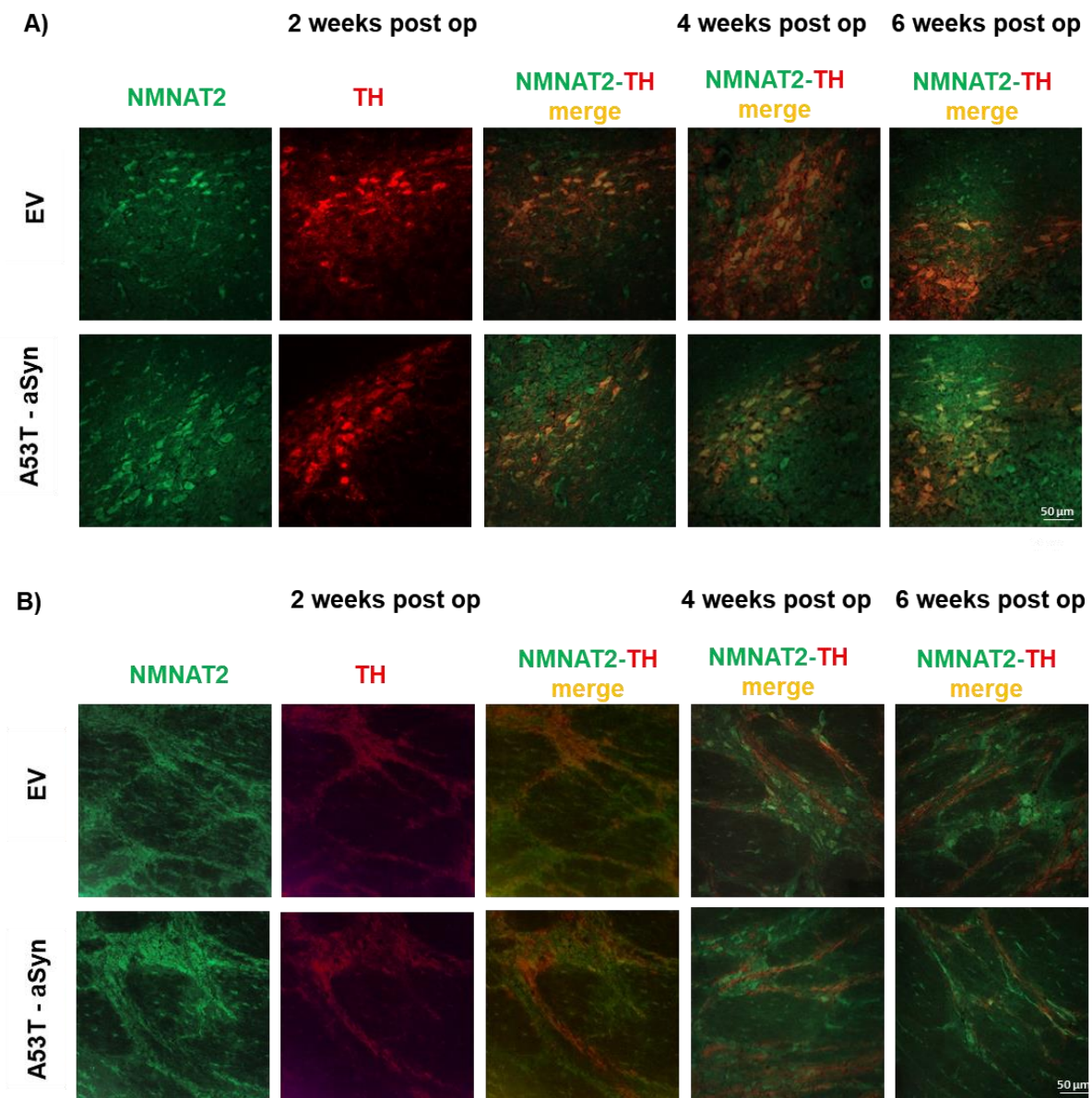


Figure 13: Immunofluorescence stainings and intensity analysis of SARM1 expression in the dopaminergic nigrostriatal tract of EV and A53T-aSyn rat groups respectively 2 weeks, 4 weeks and 6 weeks after injection.

A, B, C) Immunofluorescence stainings of SARM1 (green) and TH (red) of dopaminergic perikarya, TH-immunoreactive axons and striatal fibers in horizontal 10° rat sections 2, 4 and 6 weeks after injections, respectively. D, E, F) Immunofluorescence intensity analysis of SARM1 stainings 2, 4 and 6 weeks after injections, respectively. No evident alterations of SARM1 expression were observed in all groups.

3.10 No evident alterations of NMNAT2 expression in the nigrostriatal tract of the AAV1/2-A53T-aSyn PD rat model

No significant regulations of NMNAT2 in the nigrostriatal tract in the nigrostriatal tract in the nigrostriatal tract in the nigrostriatal tract in the nigrostriatal tract in the nigrostriatal tract in the nigrostriatal tract in the nigrostriatal tract in the nigrostriatal tract in the nigrostriatal tract in A53T-aSyn rat groups displayed comparing with EV rat groups (Figure 14).



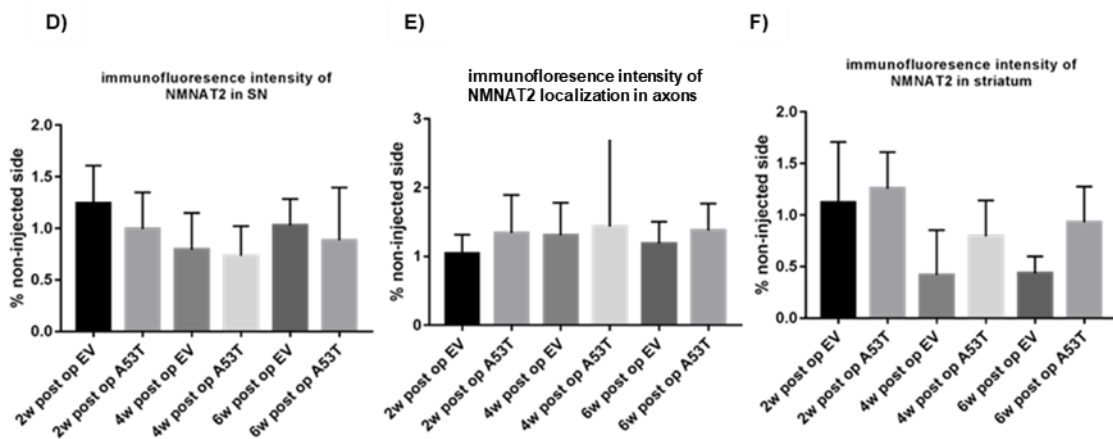
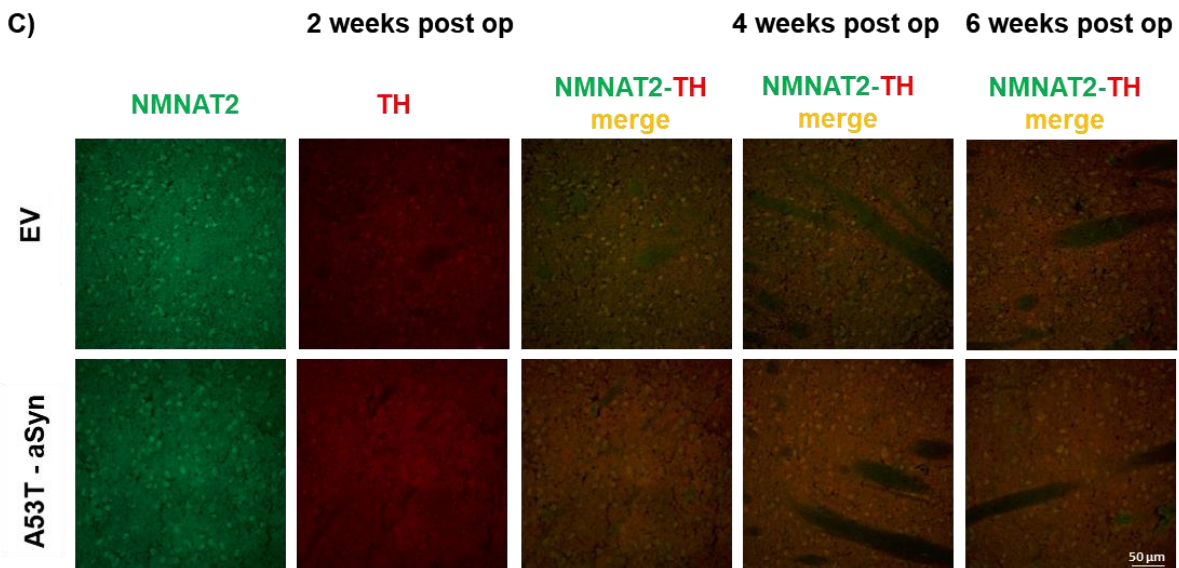


Figure 14: Immunofluorescence stainings and intensity analysis of NMNAT2 expression in the dopaminergic nigrostriatal tract of EV and A53T-aSyn rat groups respectively 2 weeks, 4 weeks and 6 weeks after injection.

A, B, C) Immunofluorescence stainings of NMNAT2 (green) and TH (red) of dopaminergic perikarya, TH-immunoreactive axons, and striatal fibers of horizontal 10° rat sections 2, 4 and 6 weeks after injections, respectively. D, E, F) Immunofluorescence intensity analysis of NMNAT2 stainings 2, 4 and 6 weeks after injections, respectively. No evident alterations of NMNAT2 expression were found in all groups.

4 Discussion

Generating an ideal PD animal model which mimics accurately human disease progression within a practical time range is an essential element in animal research. In this study our AAV1/2-induced human-mutated A53T-aSyn rat PD model developed pathological characteristics, behavioral deficits and molecular regulations of PD. One advantage of this model in the aspect of pathological feature is the presence of aSyn accumulation which is characteristic of clinical PD however not established in various PD animal models. According to our data, the AAV1/2 vector could induce A53T-aSyn overexpression from as early as 2 weeks after vector delivery into SN of the rats. At 6 weeks after AAV1/2-aSyn injections, time-dependent overexpression and distribution of A53T-aSyn along the whole nigrostriatal tract was obviously observed, showing that AAV1/2-aSyn construct is highly competent in rats in regard to covering the whole nigrostriatal pathway. Moreover, observation of the wide distribution of A53T-aSyn in the dopaminergic nigrostriatal tract confirmed the effective model induction by accurately targeting the SN of rats.

There is also advantage of our experimental method. By inventing the technology of slicing the brain section in an angle of horizontal 10°, we were able to observe and examine the pathological and molecular features on all the three important parts – SN, dopaminergic axons and striatum – of the nigrostriatal dopaminergic pathway simultaneously.

One aim of our study is to seek reliable evidence of the onset of pathological features alongside clinical parameters in PD model. For this reason, we set 3 experimental time points starting from 2 weeks which is earlier than the time points in most of the AAV-induced PD model (Koprach et al. 2011, Koprach et al. 2010). We performed two sorts of behavioral tests to detect motor deficits at respectively 2 weeks, 4 weeks and 6 weeks post injections. In addition, we carried out the examinations of a few pathological parameters, including counting of TH+ dopaminergic neurons in SN, density measurement of dopaminergic axons and TH+ fibers in the striatum on horizontal 10° sections, together with the counting of SN DA neurons on the coronal sections at the three time points. Cylinder test was applied to assess paw asymmetry of the rats. In our

assay, we found that in cylinder test starting from 2 weeks after AAV-mediated A53T-aSyn injections, slight paw asymmetry of the A53T-aSyn rat groups developed. At 4 weeks and 6 weeks post injections, paw asymmetry was more pronounced. This finding was supported by the single pellet-reaching task, which is considered a very sensitive test to examine unilateral motor dysfunction. In the single pellet-reaching task, the capacity of the contralateral paw of the A53T-aSyn rat groups to grab the pellet was slightly reduced, starting from 4 weeks, the motor function of the contralateral paw continued to worsen as time passed. At 6 weeks, we could observe a significant motor impairment comparing the A53T-aSyn groups and EV groups. Interestingly, motor deficit was accompanied by decrease of striatal terminals and DA soma in SN starting from 2 weeks and further decrease till the lowest point at 6 weeks post injection. Correlation analysis of Time-Pellet reaching reveals time-dependent progressive behavioral changes in A53T-aSyn rats.

It is important to state that in human PD cases, neurodegeneration develops broadly prior to the occurrence of motor symptoms. For example, a study by Kordower et al. stated that an estimated loss of 30% SN neurons and higher loss of dopaminergic fibers in the striatum were shown without the presence of motor deficit (Kordower et al. 2013). Opposed to the case in human disease is that in rodent models motor impairment can develop in the absence of neurodegeneration of the dopaminergic pathway (Koprach et al. 2011). In a few PD rat models, various behavioral tests have confirmed motor impairment despite the lack of dopaminergic neurodegeneration (Lee et al. 1996, Meredith & Kang 2006). These rodent PD models somehow did not completely mimic the pathophysiological features of clinical cases. In our PD model, we observed a similar phenomenon to human disease progression in the aspect that when a slight but not significant impairment of the unilateral paw started to be shown at 2 weeks time point after disease induction, neurodegeneration in the nigrostriatal tract developed. Not until 4 weeks time point did overt motor dysfunction start to appear, with a wider neurodegeneration in the nigrostriatal tract. There are a few related studies on the issue of neurodegeneration in PD, e.g. the apomorphine-induced rotational behavior of rats is associated with the degree of TH⁺ loss in the nigrostriatal pathway (Su et al. 2018).

Another PD rodent model showed progressive loss of nigral dopamine neurons starting from 8 weeks after AAV-induced wt-aSyn injection (Decressac et al. 2012).

The novelty of this study in our PD model is that pathological parameters of neurodegeneration in the nigrostriatal tract and even the motor impairment have been investigated at a time point as early as 2 weeks after model induction, which is much earlier than most of the AAV-mediated PD rodent models reported (Koprach et al. 2011, Musacchio et al. 2017). By these observations we were able to at least get a better insight into the pathological progression and the value of carrying out a therapy for PD treatment at an earlier timepoint.

Numerous research has focused on loss of dopaminergic cell bodies in PD, however some findings suggest that terminals of the dopaminergic system are involved predominantly and early in PD (Tagliaferro et al., 2016). In our experiments, a continuous decline of TH+ fiber density starting from 2 weeks was shown in both dopaminergic perikarya in SN and terminals, and dopaminergic loss reached the maximum at 6 weeks after viral vector injection. However, only loss of the dopaminergic fibers in the striatum and not of dopaminergic cell soma correlates significantly with motor dysfunction. This observation could explain the terminal neurodegeneration better than the loss of dopaminergic cell soma. It provides insights that dopaminergic axonal degeneration precedes cell soma degeneration in our A53T-aSyn PD model. This observation is in line with the previously published data. In a MPTP macaque model of PD, a significant reduction of dopaminergic axons prior to the degeneration of cell soma was found (Meissner et al., 2003). Unexpectedly, a slight trend instead of significant decline of TH+ density of dopaminergic axons was found in A53T-aSyn rats. We speculate that it might attribute to the technical difficulty of exactly cutting the long dopaminergic axons in a longitudinal fashion, which impacts the accuracy of analysis. Thus the axonal data have to be taken with a grain of salt. Since a clear loss of dopaminergic cell bodies and striatal terminals was observed, future examination of the dopaminergic axons employing more applicable method is meaningful.

Importantly, for all the examinations stated above, including density measurement of the whole dopaminergic nigrostriatal pathway and the SN cell loss by Stereology

counting, the alterations occur in a time-dependent manner starting from 2 weeks till 6 weeks, indicating a time-dependent progressive neurodegeneration after AAV mediated A53T-aSyn expression.

Up till now no causative therapy has been confirmed for the treatment of PD. The therapeutic effects of PD remain challenging. Thus seeking novel therapeutic biomarkers is imperative. Recently, extensive studies have emphasized the essential role of pro- and antidegeneration markers playing in neurodegenerative disease (Ali et al. 2016, Meng et al. 2017, Pinho et al. 2016, Zhang et al. 2018). However the relation of these molecules with PD has not been thoroughly demonstrated. Moreover, most previous experiments were either designed to detect the overall expression of the pro- and antidegeneration markers in the nigrostriatal tract using western blot (WB) method or PCR, without the possibility to visualize the expression of these biomarkers in each single structure of the nigrostriatal tract, or the experiments were aimed at DA cell bodies in SN, without paying enough attention to the long and vulnerable dopaminergic axons. In this study, we sliced the rat brain in an angle of horizontal 10° so that all the three important parts – SN, dopaminergic axons and striatum – of the nigrostriatal dopaminergic pathway could be observed and examined simultaneously. Different from most of the aforementioned experiments, we employed immunohistochemistry method on this study to detect the pro- and antidegeneration markers. By performing fluorescence double stainings of these molecules with TH, we were able to visualize the location of the molecules in TH+ DA cell along the nigrostriatal pathway on the horizontal 10° rat brain section. From the fluorescence images we were able to observe the expressions of the pro- and antidegeneration markers in the SN perikarya clearly. However from the axon bundles presented in the images it is difficult to ascertain that the staining for the molecules really shows signals inside the nigrostriatal dopaminergic axons. There is possibility that as the dot-like staining pattern of the molecules in the axons belong to cell bodies of other neural pathways passing through the location of the nigrostriatal dopaminergic axons. We observed that all the 4 molecules that were intended to be explored were widely distributed in the SN and dopaminergic axons. Although we are aware that the signals of the molecules may not specifically stand for the dopaminergic axons, at least the intensity of the molecules in the TH- axons measured in our analysis

which includes both the TH-positive axon bundles and the dot-like staining could indicate a trend of expression change inside the nigrostriatal dopaminergic axons. As for the case in the striatum, for the reason that there are a type of TH+ positive interneurons in the striatum, and that countless stripes and various types of cells are filled in the striatum which makes it difficult to differentiate if the staining of the molecules is in the dopaminergic terminal or located in another cell type, we failed to detect any reliable alterations of the molecules in the dopaminergic fibers in the striatum by performing immunofluorescence method. However future explorations of administering a proper experimental method e.g. Western blot or PCR for the examinations of the molecules in the striatum should be carried out.

As a nuclear transcription factor, Nrf2 plays the main regulatory role in antioxidant defense. As aforementioned study showed, under physiological conditions the antioxidant enzymes whose transcription are regulated by Nrf2 exert a neuroprotective role on DA neurons (Meng et al. 2017). However when influenced by pathological factors, such as MPTP, rotenone or other pathogenic factors, Nrf2 would be transported to the axons and lead to decreased nuclear localization and thus decreased neuroprotection, which in turn negatively affects the ability to prevent against oxidant damage. However in another study, Ramsey et. al found that Nrf2 nuclear signal was abundantly stronger in surviving neurons compared with control groups (Ramsey et al. 2007). Despite these discrepant reports, we investigated a progressive trend of decrease of Nrf2 expression in both SN and TH-immunoreactive axons, at 6 weeks after PD model induction a significant decline was observed, suggesting a reduced ability to react to oxidative damage. This discovery is similar to a previous finding that showed an overall decline of Nrf2 expression in dopaminergic neurons (Meng et al. 2017). In our experiment, we were able to detect the exact alteration of Nrf2 expression separately in DA cell body in SN and in the TH-immunoreactive axon bundles. In another study, Ramsey et. al found that Nrf2 nuclear signal was abundantly stronger in surviving neurons compared with control groups. This may be because nuclear translocate of Nrf2 delayed neuron damage. However in the neurons which have been lost after oxidative stress, Nrf2 may not be sufficient to prevent neuronal damage, presumably due to insufficient ability of Nrf2 to respond to oxidative stress or failed nuclear transport of Nrf2 (Ramsey et al. 2007). This

phenomenon indicates the protective function of Nrf2 in DA neurons. Thus, lack of Nrf2 may directly result in damaged antioxidant response in PD. Dr. T. Musacchio and Fabian Kremer performed immunofluorescence intensity analysis of Nrf2 with the same PD model, they found a slightly but not significantly elevated nucleo-cytoplasmic ratio of Nrf2 expression in A53T-aSyn PD rats. In all, Nrf2 may participate in the pathogenesis of PD but not a key factor in degeneration of dopaminergic neurons in the A53T-aSyn PD model.

Another molecule Tau, has been largely characterized to be a common pathophysiological feature in AD and PD (Moussaud et al. 2014, Zhang et al. 2018). Tau has been characterized to be over-phosphorylated and then accumulate in the axoplasm and interfere with axonal cytoskeleton which damages axons. Similar to the case of Nrf2, Tau has also been reported to transfer from the nucleus to axoplasm under pathological conditions. In our PD model, we found a slight decline of Tau expression in SN starting from 2 weeks after disease model induction, whereas a respectively evident trend of upregulation overtime in the dopaminergic axons. Similar to our observation, Li and colleagues detected that neurofibrillary tangles composed mainly of misfolded tau spread along the neuronal pathways (Li et al. 2008). As aforementioned, recently mounting evidence suggest that asyn and tau interact and this interaction essentially contribute to the development and spread of neurodegeneration (Arima et al. 1999, Duda et al. 2002, Moussaud et al. 2014). Thus, one explanation to tau alterations in this study is that A53T-asyn injection leads to increased phosphorylated tau levels. The phosphorylated tau would be transported to the axons and accumulate in an aggregated form which result in axonal degeneration. Moreover, under pathological conditions in PD tau is considered to separate from microtubule which future damages the axons (Arai et al. 2001). As for the question why tau upregulation in the axons is not significant, we presume that the level of A53T-asyn overexpression in the dopaminergic tract and time phrase after A53T-asyn overexpression to develop pathology largely limits the level of tau aggregation. Another reason might be that, as described in the last paragraph, the staining of molecules in the location of axons do not really specifically show signals in the nigrostriatal dopaminergic axons, but other neural pathways. Thus future experimental method like high resolution microscopy should be used to better

address the question. A few other viral vector-based models also showed tight correlation between A53T-*syn* overexpression and increased phospho-tau levels (Khandelwal et al. 2010). In an experiment using adeno-associated vectors for gene transfer into the SN of rats, overexpression of tau was confirmed to provoke dopaminergic neurodegeneration and induce motor dysfunction (Klein et al. 2005). For the slight decrease of Tau in SN, one explanation might be that tau is transported to the dopaminergic axons.

Based on the above descriptions that regulations of Tau expression in PD are associated with nucleus transport, we conclude that inhibitors of nucleus transporters might be promising candidates to attenuate neuronal damage. Further research needs to be done on this topic.

We investigated the expression of NMNAT2 in our PD rat model, to gain insights into their role in the viral-vector induced PD model and how it plays its role. As the published data described, NMNAT2 and NMNAT2 mRNA level were reduced in human PD models (Ali et al. 2016). Unexpectedly, in our PD model using immunofluorescence method, no evident alterations or change of trend of NMNAT2 was observed in both SN and the dopaminergic axons. Thus this AAV1/2-A53T-*aSyn* induced rat PD model may be of little relevance for the investigation of NMNAT2 protein. Nonetheless, employing various experimental methods such as WB or PCR to detect the NMNAT2 mRNA would be helpful to confirm our observations in this study. Similar to the observation of NMNAT2, we could not detect any meaningful changes of SARM1 in our AAV1/2-A53T-*aSyn* rat PD model. Interestingly, SARM1 and NMNAT1 have been considerably described to interact with each other (Conforti et al. 2014) and they function in a NMN-SARM1 dependent way in Wallerian degeneration (Loreto et al. 2015). Thus it is reasonable to assume these two molecules might also act in a similar pattern in retrograde degeneration in PD. This is also consistent with our findings that neither NMNAT1 nor SARM1 is regulated in this PD rat model. It has been considered that targeting Sarm1 to block axonal degeneration is a promising access (Murata et al. 2013). As to date there are few reported studies about the association of SARM1 and PD reported, future research relating SARM1 and PD is imperative.

Since the pathological features of human PD disease, like aSyn accumulation, motor impairment and nigrostriatal degeneration have been verified in this AAV1/2 A53T rat model, we propose that the predictive validity and translational value are ascertained. Thus, we suggest applications of molecular targets to relieve neurodegeneration in PD. Nrf2 might act as a neuroprotective role in PD rats but not an essential player in degeneration of dopaminergic neurons in the aSyn PD model, at least not in the here described stage of disease. As for SARM1 and NMNAT2 which are not found to be altered in our PD model, we presume these two molecules probably have no effect on the pathological process in our PD model. However future research is needed to exclude SARM1 and NMNAT2 as candidate for therapeutic targets for PD.

5 Conclusion

Employing an appropriate animal model is imperative for PD study. In spite of mounting PD animal models occurring in recent years, few of them has thoroughly exemplified the disease in all the key aspects. In this study, our AAV-A53T rat model has successfully induced the neuropathological hallmarks and clinical features of PD, thus has an advantage over previous PD animal models in disease predictability.

To get a better insight into the issue of onset time point of PD which may contribute to answering the question whether earlier intervention of PD is vital, we carried out behavioral investigation coupled with pathological characterization in this PD model starting from an early time point to respectively late time points. In two types of behavioral tests, we have observed a time-dependent impairment of the motor functions starting from 2 weeks which is much earlier than the start time point of current treatment for PD. With stereological analysis, we also discovered that neurodegeneration of the nigrostriatal tract in this AAV1/2-A53T-aSyn rat model started from as early as 2 weeks, which is in accordance with the result in behavioral examinations. What is more, loss of the terminals correlated significantly with motor deficits in aSyn PD rats. Thus earlier intervention of PD may be a possible insight in treating PD.

For the question from which part of the nigrostriatal tract does neurodegeneration start, we performed optical density analysis on the angel sections on which the whole nigrostriatal pathway could be visualized. We found a significant loss of dopaminergic perikarya in SN and terminals in the striatum in the A53T-aSyn rat model as early as four weeks after viral vector injection. However, only loss of the dopaminergic terminals and not of cell soma correlated significantly with motor dysfunction in A53T-aSyn PD rats. This observation emphasizes the important role of axonopathy in this A53T-aSyn PD model.

With a growing interest in exploring the role of pro- and antidegeneration markers in PD these years, we implemented investigations for a few pro- and antidegeneration markers associated with aSyn function or PD (Table 1). With immunofluorescence stainings and fluorescence intensity analysis, we showed that Nrf2 is downregulated in

DA neurons in SN and in TH-immunoreactive axons, probably causing insufficient oxidative response to pathological factors in PD progression. In the experiment performed by Dr. T. Musacchio and Fabian Kremer with the same PD rat model, no significant changes were found comparing the nucleo-cytoplasmic ratio of A53T-aSyn PD rats with controls for Nrf2, thus Nrf2 may not be regarded as a valuable therapeutic molecular target in this PD rat model. In addition, we observed a slight but nonsignificant downregulation of Tau in DA neurons in SN but nonsignificant upregulation in dopaminergic axons. However, further study has yet to determine if Tau can be transported to the axons and aggregates by interacting with aSyn and thus disrupts cytoskeleton structures under pathophysiological conditions in PD. Lastly, no alterations of SARM1 and NMNAT2 were found in this PD model, indicating little relevance of these three pro- and antidegeneration markers with our AAV1/2-A53T-aSyn rat model. These results gave new insights on the potential biomarkers disease of PD.

There are some other limitations in this study. Firstly, reversible treatments (e.g. L-DOPA) of motor dysfunction in our PD model were not performed thus limiting the translational validity of this model. Secondly, no control groups that could produce a control protein in comparison with A53T protein were accomplished in this experiment. However in the earlier study reported by Koprach et al. using the same type of viral vector in a PD rat model, the AAV1/2-induced green fluorescent protein as a control protein has produced neurodegeneration to some extent, but significantly less than comparing with AAV1/2-induced A53T protein. Last but not least, neither treatment nor interventional experiments in our PD model have been conducted because of time and sample limits. Thus further studies to apply for a specific therapeutic method, or to administrate inhibitors of the pro- and antidegeneration markers assessed in our experiments (Nrf2, Tau, SARM1 and NMNAT2) or to induce knock out rats of the described pro- and antidegeneration markers in this AAV1/2 A53T-aSyn rat PD model are needed, for the purpose of exploring the value of these molecules as therapeutic targets.

Table 1: Alterations of pro- and antidegeneration markers (Nrf2, Tau, SARM1 and NMNAT2) in the nigrostriatal tract in the AAV1/2-A53T-aSyn rat PD model.

Pro- and <u>antidegeneration</u> markers	Regulation in SN	Regulation in axon localization	Regulation in striatum
Nrf2	↓ *	↓ *	?
Tau	↓	↑	?
SARM1	—	—	?
NMNAT2	—	—	?

6 Reference

- Abeliovich A, Gitler AD. 2016. Defects in trafficking bridge Parkinson's disease pathology and genetics. *Nature* 539: 207-16
- Ahuja M, Ammal Kaidery N, Yang L, Calingasan N, Smirnova N, et al. 2016. Distinct Nrf2 Signaling Mechanisms of Fumaric Acid Esters and Their Role in Neuroprotection against 1-Methyl-4-Phenyl-1,2,3,6-Tetrahydropyridine-Induced Experimental Parkinson's-Like Disease. *36*: 6332-51
- Alfieri A, Srivastava S, Siow RC, Mudo M, Fraser PA, Mann GE. 2011. Targeting the Nrf2-Keap1 antioxidant defence pathway for neurovascular protection in stroke. *The Journal of physiology* 589: 4125-36
- Ali YO, Allen HM, Yu L, Li-Kroeger D, Bakhshizadehmahmoudi D. 2016. NMNAT2:HSP90 Complex Mediates Proteostasis in Proteinopathies. *14*: e1002472
- Alonso A, Zaidi T, Novak M, Grundke-Iqbal I, Iqbal K. 2001. Hyperphosphorylation induces self-assembly of tau into tangles of paired helical filaments/straight filaments. *Proceedings of the National Academy of Sciences of the United States of America* 98: 6923-8
- Ammal Kaidery N, Tarannum S, Thomas B. 2013. Epigenetic landscape of Parkinson's disease: emerging role in disease mechanisms and therapeutic modalities. *Neurotherapeutics : the journal of the American Society for Experimental NeuroTherapeutics* 10: 698-708
- Anna O, Wojciech K, Margarita L, Jolanta D. 2013. Mutations in PRKN and SNCA Genes Important for the Progress of Parkinson's Disease. *Current Genomics* 14: -
- Appel-Cresswell S, Vilarino-Guell C, Encarnacion M, Sherman H, Yu I, et al. 2013. Alpha-synuclein p.H50Q, a novel pathogenic mutation for Parkinson's disease. *Movement disorders : official journal of the Movement Disorder Society* 28: 811-3
- Arai T, Ikeda K, Akiyama H, Shikamoto Y, Tsuchiya K, et al. 2001. Distinct isoforms of tau aggregated in neurons and glial cells in brains of patients with Pick's disease, corticobasal degeneration and progressive supranuclear palsy. *Acta neuropathologica* 101: 167-73
- Arima K, Hirai S, Sunohara N, Aoto K, Izumiyama Y, et al. 1999. Cellular co-localization of phosphorylated tau- and NACP/alpha-synuclein-epitopes in Lewy bodies in sporadic Parkinson's disease and in dementia with Lewy bodies. *Brain research* 843: 53-61
- Armstrong RA, Cairns NJ. 2013. Spatial patterns of the tau pathology in progressive supranuclear palsy. *Neurological sciences : official journal of the Italian Neurological Society and of the Italian Society of Clinical Neurophysiology* 34: 337-44
- Ball N, Teo WP, Chandra S, Chapman J. 2019. Parkinson's Disease and the Environment. *Frontiers in neurology* 10: 218
- Betarbet R, Sherer TB, MacKenzie G, Garcia-Osuna M, Panov AV, Greenamyre JT. 2000. Chronic systemic pesticide exposure reproduces features of Parkinson's disease. *Nature neuroscience* 3: 1301-6
- Blesa J, Przedborski S. 2014. Parkinson's disease: animal models and dopaminergic cell vulnerability. *Frontiers in neuroanatomy* 8: 155
- Bosch C, Mailly P, Degos B, Deniau JM, Venance L. 2012. Preservation of the hyperdirect pathway of basal ganglia in a rodent brain slice. *Neuroscience* 215: 31-41
- Bottner M, Fricke T, Muller M, Barrenschee M, Deuschl G, et al. 2015. Alpha-synuclein is associated with the synaptic vesicle apparatus in the human and rat enteric nervous system. *Brain research* 1614: 51-9
- Bourdenx M, Dovero S, Engeln M, Bido S, Bastide MF, et al. 2015. Lack of additive role of ageing in nigrostriatal neurodegeneration triggered by alpha-synuclein overexpression. *Acta neuropathologica communications* 3: 46

- Bove J, Prou D, Perier C, Przedborski S. 2005. Toxin-induced models of Parkinson's disease. *NeuroRx : the journal of the American Society for Experimental NeuroTherapeutics* 2: 484-94
- Bridi JC, Hirth F. 2018. Mechanisms of alpha-Synuclein Induced Synaptopathy in Parkinson's Disease. *Frontiers in neuroscience* 12: 80
- Brion JP, Couck AM, Passareiro E, Flament-Durand J. 1985. Neurofibrillary tangles of Alzheimer's disease: an immunohistochemical study. *Journal of submicroscopic cytology* 17: 89-96
- Burton GJ, Jauniaux E. 2011. Oxidative stress. *Best practice & research. Clinical obstetrics & gynaecology* 25: 287-99
- Cacabelos R. 2017. Parkinson's Disease: From Pathogenesis to Pharmacogenomics. *International journal of molecular sciences* 18
- Calabresi P, Picconi B, Tozzi A, Ghiglieri V, Di Filippo M. 2014. Direct and indirect pathways of basal ganglia: a critical reappraisal. *Nature neuroscience* 17: 1022-30
- Carvalho GA, Nikkhah G. 2001. Subthalamic nucleus lesions are neuroprotective against terminal 6-OHDA-induced striatal lesions and restore postural balancing reactions. *Experimental neurology* 171: 405-17
- Cenci MA, Whishaw IQ, Schallert T. 2002. Animal models of neurological deficits: how relevant is the rat? *Nature reviews. Neuroscience* 3: 574-9
- Cha JH. 2000. Transcriptional dysregulation in Huntington's disease. *Trends in neurosciences* 23: 387-92
- Chai C, Lim K-L. 2013. Genetic insights into sporadic Parkinson's disease pathogenesis. *Current genomics* 14: 486-501
- Chartier-Harlin MC, Kachergus J, Roumier C, Mouroux V, Douay X, et al. 2004. Alpha-synuclein locus duplication as a cause of familial Parkinson's disease. *Lancet (London, England)* 364: 1167-9
- Chen CY, Lin CW, Chang CY, Jiang ST, Hsueh YP. 2011. Sarm1, a negative regulator of innate immunity, interacts with syndecan-2 and regulates neuronal morphology. *The Journal of cell biology* 193: 769-84
- Chiu S, Terpstra KJ, Bureau Y, Hou J, Raheb H, et al. 2013. Liposomal-formulated curcumin [Lipocurc] targeting HDAC (histone deacetylase) prevents apoptosis and improves motor deficits in Park 7 (DJ-1)-knockout rat model of Parkinson's disease: implications for epigenetics-based nanotechnology-driven drug platform. *Journal of complementary & integrative medicine* 10
- Chu Y, Morfini GA, Kordower JH. 2016. Alterations in Activity-Dependent Neuroprotective Protein in Sporadic and Experimental Parkinson's Disease. *Journal of Parkinson's disease* 6: 77-97
- Chuang CF, Bargmann CI. 2005. A Toll-interleukin 1 repeat protein at the synapse specifies asymmetric odorant receptor expression via ASK1 MAPKKK signaling. *Genes & development* 19: 270-81
- Clark IE, Dodson MW, Jiang C, Cao JH, Huh JR, et al. 2006. Drosophila pink1 is required for mitochondrial function and interacts genetically with parkin. *Nature* 441: 1162-66
- Cobley JN, Fiorello ML, Bailey DM. 2018. 13 reasons why the brain is susceptible to oxidative stress. *Redox biology* 15: 490-503
- Collier TJ, Kanaan NM, Kordower JH. 2011. Ageing as a primary risk factor for Parkinson's disease: evidence from studies of non-human primates. *Nature reviews. Neuroscience* 12: 359-66
- Conforti L, Gilley J, Coleman MP. 2014. Wallerian degeneration: an emerging axon death pathway linking injury and disease. *Nature reviews. Neuroscience* 15: 394-409

- Costa CA, Da, Ancolio K, ., Checler F, . 2000. Wild-type but not Parkinson's disease-related alpha-53 --> Thr mutant alpha-synuclein protects neuronal cells from apoptotic stimuli. *Journal of Biological Chemistry* 275: 24065-69
- Creed RB, Goldberg MS. 2018. New Developments in Genetic rat models of Parkinson's Disease. *Movement disorders : official journal of the Movement Disorder Society* 33: 717-29
- Daher JP, Volpicelli-Daley LA, Blackburn JP, Moehle MS, West AB. 2014. Abrogation of alpha-synuclein-mediated dopaminergic neurodegeneration in LRRK2-deficient rats. *Proceedings of the National Academy of Sciences of the United States of America* 111: 9289-94
- Dauer W, Przedborski S. 2003. Parkinson's disease: mechanisms and models. *Neuron* 39: 889-909
- Dave KD, De Silva S, Sheth NP, Ramboz S, Beck MJ, et al. 2014. Phenotypic characterization of recessive gene knockout rat models of Parkinson's disease. *Neurobiology of disease* 70: 190-203
- De Vos KJ, Grierson AJ, Ackerley S, Miller CC. 2008. Role of axonal transport in neurodegenerative diseases. *Annual review of neuroscience* 31: 151-73
- Decressac M, Mattsson B, Lundblad M, Weikop P, Bjorklund A. 2012. Progressive neurodegenerative and behavioural changes induced by AAV-mediated overexpression of alpha-synuclein in midbrain dopamine neurons. *Neurobiology of disease* 45: 939-53
- Delcuve GP, Khan DH, Davie JR. 2012. Roles of histone deacetylases in epigenetic regulation: emerging paradigms from studies with inhibitors. *Clinical epigenetics* 4: 5
- Di Monte DA. 2003. The environment and Parkinson's disease: is the nigrostriatal system preferentially targeted by neurotoxins? *The Lancet. Neurology* 2: 531-8
- Di Stefano M, Conforti L. 2013. Diversification of NAD biological role: the importance of location. *The FEBS journal* 280: 4711-28
- Doherty KM, Hardy J. 2013. Parkin disease and the Lewy body conundrum. *Movement disorders : official journal of the Movement Disorder Society* 28: 702-4
- Dringen R, Pfeiffer B, Hamprecht B. 1999. Synthesis of the antioxidant glutathione in neurons: supply by astrocytes of CysGly as precursor for neuronal glutathione. *The Journal of neuroscience : the official journal of the Society for Neuroscience* 19: 562-9
- Duda JE, Giasson BI, Mabon ME, Miller DC, Golbe LI, et al. 2002. Concurrence of alpha-synuclein and tau brain pathology in the Contursi kindred. *Acta neuropathologica* 104: 7-11
- Eriksen JL, Dawson TM, Dickson DW, Petrucelli L. 2003. Caught in the act: alpha-synuclein is the culprit in Parkinson's disease. *Neuron* 40: 453-6
- Exner N, Lutz AK, Haass C, Winklhofer KF. 2012. Mitochondrial dysfunction in Parkinson's disease: molecular mechanisms and pathophysiological consequences. *The EMBO journal* 31: 3038-62
- Fang Y, Soares L, Teng X, Geary M, Bonini NM. 2012. A novel Drosophila model of nerve injury reveals an essential role of Nmnat in maintaining axonal integrity. *Current biology : CB* 22: 590-5
- Faull RL, Lavery R. 1969. Changes in dopamine levels in the corpus striatum following lesions in the substantia nigra. *Experimental neurology* 23: 332-40
- Funayama M, Li Y, Tsoi TH, Lam CW, Ohi T, et al. 2008. Familial Parkinsonism with digenic parkin and PINK1 mutations. *Movement disorders : official journal of the Movement Disorder Society* 23: 1461-5
- Galpern WR, Lang AE. 2006. Interface between tauopathies and synucleinopathies: a tale of two proteins. *Annals of neurology* 59: 449-58

- Gamache P-L, Roux-Dubois N, Provencher P, Lebouthiller J, Gan-Or Z, Dupre N. 2017. Professional exposure to pesticides and heavy metals hastens Parkinson Disease onset (P6.008). *Neurology* 88: P6.008
- Gandhi S, Wood-Kaczmar A, Yao Z, Plun-Favreau H, Deas E, et al. 2009. PINK1-associated Parkinson's disease is caused by neuronal vulnerability to calcium-induced cell death. *Molecular cell* 33: 627-38
- Garbarino VR, Orr ME, Rodriguez KA, Buffenstein R. 2015. Mechanisms of oxidative stress resistance in the brain: Lessons learned from hypoxia tolerant extremophilic vertebrates. *Arch Biochem Biophys* 576: 8-16
- Gerdts J, Summers DW, Sasaki Y, DiAntonio A, Milbrandt J. 2013. Sarm1-mediated axon degeneration requires both SAM and TIR interactions. *The Journal of neuroscience : the official journal of the Society for Neuroscience* 33: 13569-80
- Gilley J, Adalbert R, Yu G, Coleman MP. 2013. Rescue of peripheral and CNS axon defects in mice lacking NMNAT2. *The Journal of neuroscience : the official journal of the Society for Neuroscience* 33: 13410-24
- Gilley J, Coleman MP. 2010. Endogenous Nmnat2 is an essential survival factor for maintenance of healthy axons. *PLoS biology* 8: e1000300
- Gitler AD, Dhillon P, Shorter J. 2017. Neurodegenerative disease: models, mechanisms, and a new hope. 10: 499-502
- Golbe LI, Di Iorio G, Bonavita V, Miller DC, Duvoisin RC. 1990. A large kindred with autosomal dominant Parkinson's disease. *Annals of neurology* 27: 276-82
- Goldberg MS, Pisani A, Haburcak M, Vortherms TA, Kitada T, et al. 2005. Nigrostriatal dopaminergic deficits and hypokinesia caused by inactivation of the familial Parkinsonism-linked gene DJ-1. *Neuron* 45: 489-96
- Grant LM, Kelm-Nelson CA, Hilby BL, Blue KV, Paul Rajamanickam ES, et al. 2015. Evidence for early and progressive ultrasonic vocalization and oromotor deficits in a PINK1 gene knockout rat model of Parkinson's disease. *Journal of neuroscience research* 93: 1713-27
- Hashimoto M, Masliah E. 1999. Alpha-synuclein in Lewy body disease and Alzheimer's disease. *Brain pathology (Zurich, Switzerland)* 9: 707-20
- Haines, J. D. , Herbin, O. , DLH Belén, Vidaurre, O. G. , Moy, G. A. , & Sun, Q. , et al. 2015. Nuclear export inhibitors avert progression in preclinical models of inflammatory demyelination. *Nature Neuroence* 18(4), 511-20.
- Hattori N, ., Kitada T, ., Matsumine H, ., Asakawa S, ., Yamamura Y, ., et al. 1998. Molecular genetic analysis of a novel Parkin gene in Japanese families with autosomal recessive juvenile parkinsonism: evidence for variable homozygous deletions in the Parkin gene in affected individuals. *Annals of neurology* 44: 935-41
- Hayes JD, Dinkova-Kostova AT. 2014. The Nrf2 regulatory network provides an interface between redox and intermediary metabolism. *Trends in biochemical sciences* 39: 199-218
- He Q, Koprach JB, Wang Y, Yu WB, Xiao BG, et al. 2016. Treatment with Trehalose Prevents Behavioral and Neurochemical Deficits Produced in an AAV alpha-Synuclein Rat Model of Parkinson's Disease. *Molecular neurobiology* 53: 2258-68
- Healy DG, Mario F, O'Sullivan SS, Vincenzo B, Alexandra D, et al. 2008. Phenotype, genotype, and worldwide genetic penetrance of LRRK2-associated Parkinson's disease: a case-control study. *Lancet Neurology* 7: 583-90
- Hedrich K, Eskelson C, Wilmot B, Marder K, Harris J, et al. 2004. Distribution, type, and origin of Parkin mutations: review and case studies. *Movement disorders : official journal of the Movement Disorder Society* 19: 1146-57

- Hicks AN, Lorenzetti D, Gilley J, Lu B, Andersson KE, et al. 2012. Nicotinamide mononucleotide adenylyltransferase 2 (Nmnat2) regulates axon integrity in the mouse embryo. *PLoS one* 7: e47869
- Ip CW, Klaus LC, Karikari AA, Visanji NP, Brotchie JM, et al. 2017. AAV1/2-induced overexpression of A53T-alpha-synuclein in the substantia nigra results in degeneration of the nigrostriatal system with Lewy-like pathology and motor impairment: a new mouse model for Parkinson's disease. *Acta neuropathologica communications* 5: 11
- Irwin DJ, Lee VM, Trojanowski JQ. 2013. Parkinson's disease dementia: convergence of alpha-synuclein, tau and amyloid-beta pathologies. *Nature reviews. Neuroscience* 14: 626-36
- Irwin M, Moos W, Faller D, Steliou K, Pinkert C. 2016. *Epigenetic Treatment of Neurodegenerative Disorders: Alzheimer and Parkinson Diseases*. n/a-n/a pp.
- Itoh K, Wakabayashi N, Katoh Y, Ishii T, Igarashi K, et al. 1999. Keap1 represses nuclear activation of antioxidant responsive elements by Nrf2 through binding to the amino-terminal Neh2 domain. *Genes & development* 13: 76-86
- Itoh K, Wakabayashi N, Katoh Y, Ishii T, O'Connor T, Yamamoto M. 2003. Keap1 regulates both cytoplasmic-nuclear shuttling and degradation of Nrf2 in response to electrophiles. *Genes to cells : devoted to molecular & cellular mechanisms* 8: 379-91
- Javitch JA, D'Amato RJ, Strittmatter SM, Snyder SH. 1985. Parkinsonism-inducing neurotoxin, N-methyl-4-phenyl-1,2,3,6 -tetrahydropyridine: uptake of the metabolite N-methyl-4-phenylpyridine by dopamine neurons explains selective toxicity. *Proceedings of the National Academy of Sciences of the United States of America* 82: 2173-7
- Jellinger KA. 2011. Interaction between alpha-synuclein and tau in Parkinson's disease comment on Wills et al.: elevated tauopathy and alpha-synuclein pathology in postmortem Parkinson's disease brains with and without dementia. *Exp Neurol* 2010; 225: 210-218. *Experimental neurology* 227: 13-8
- Jenner P. 2003. Oxidative stress in Parkinson's disease. *Annals of neurology* 53 Suppl 3: S26-36; discussion S36-8
- Jiang C, Wan X, Jankovic J, Christian ST, Pristupa ZB, et al. 2004. Dopaminergic properties and experimental anti-parkinsonian effects of IPX750 in rodent models of Parkinson disease. *Clinical neuropharmacology* 27: 63-73
- Johnson JA, Johnson DA, Kraft AD, Calkins MJ, Jakel RJ, et al. 2008. The Nrf2-ARE pathway: an indicator and modulator of oxidative stress in neurodegeneration. *Annals of the New York Academy of Sciences* 1147: 61-9
- Khandelwal PJ, Dumanis SB, Feng LR, Maguire-Zeiss K, Rebeck G, et al. 2010. Parkinson-related parkin reduces α -Synuclein phosphorylation in a gene transfer model. *Molecular neurodegeneration* 5: 47
- Kim CY, Alcalay RN. 2017. Genetic Forms of Parkinson's Disease. *Seminars in neurology* 37: 135-46
- Kim S, Seo JH, Suh YH. 2004. Alpha-synuclein, Parkinson's disease, and Alzheimer's disease. *Parkinsonism & related disorders* 10 Suppl 1: S9-13
- Kim Y, Zhou P, Qian L, Chuang JZ, Lee J, et al. 2007. MyD88-5 links mitochondria, microtubules, and JNK3 in neurons and regulates neuronal survival. *The Journal of experimental medicine* 204: 2063-74
- Kirik D, Rosenblad C, Burger C, Lundberg C, Johansen TE, et al. 2002. Parkinson-like neurodegeneration induced by targeted overexpression of alpha-synuclein in the nigrostriatal system. *The Journal of neuroscience : the official journal of the Society for Neuroscience* 22: 2780-91
- Klein RL, Dayton RD, Lin WL, Dickson DW. 2005. Tau gene transfer, but not alpha-synuclein, induces both progressive dopamine neuron degeneration and rotational behavior in the rat. *Neurobiology of disease* 20: 64-73

- Klein RL, King MA, Hamby ME, Meyer EM. 2002. Dopaminergic cell loss induced by human A30P alpha-synuclein gene transfer to the rat substantia nigra. *Human gene therapy* 13: 605-12
- Koenekoop RK, Wang H, Majewski J, Wang X, Lopez I, et al. 2012. Mutations in NMNAT1 cause Leber congenital amaurosis and identify a new disease pathway for retinal degeneration. *Nature genetics* 44: 1035-9
- Koprich JB, Johnston TH, Huot P, Reyes MG, Espinosa M, Brotchie JM. 2011. Progressive neurodegeneration or endogenous compensation in an animal model of Parkinson's disease produced by decreasing doses of alpha-synuclein. *PloS one* 6: e17698
- Koprich JB, Johnston TH, Reyes MG, Sun X, Brotchie JM. 2010. Expression of human A53T alpha-synuclein in the rat substantia nigra using a novel AAV1/2 vector produces a rapidly evolving pathology with protein aggregation, dystrophic neurite architecture and nigrostriatal degeneration with potential to model the pathology of Parkinson's disease. *Molecular neurodegeneration* 5: 43
- Koprich JB, Kalia LV, Brotchie JM. 2017. Animal models of alpha-synucleinopathy for Parkinson disease drug development. *Nature reviews. Neuroscience* 18: 515-29
- Kordower JH, Olanow CW, Dodiya HB, Chu Y, Beach TG, et al. 2013. Disease duration and the integrity of the nigrostriatal system in Parkinson's disease. *Brain : a journal of neurology* 136: 2419-31
- Kruger R, Kuhn W, Muller T, Woitalla D, Graeber M, et al. 1998. Ala30Pro mutation in the gene encoding alpha-synuclein in Parkinson's disease. *Nature genetics* 18: 106-8
- Kurup PK, Xu J, Videira RA, Ononenyi C, Baltazar G, et al. 2015. STEP61 is a substrate of the E3 ligase parkin and is upregulated in Parkinson's disease. *Proceedings of the National Academy of Sciences of the United States of America* 112: 1202-7
- Leao AH, Sarmiento-Silva AJ, Santos JR, Ribeiro AM, Silva RH. 2015. Molecular, Neurochemical, and Behavioral Hallmarks of Reserpine as a Model for Parkinson's Disease: New Perspectives to a Long-Standing Model. *Brain pathology (Zurich, Switzerland)* 25: 377-90
- Lee CS, Sauer H, Bjorklund A. 1996. Dopaminergic neuronal degeneration and motor impairments following axon terminal lesion by intrastriatal 6-hydroxydopamine in the rat. *Neuroscience* 72: 641-53
- Lee JW, Tapias V, Di Maio R, Greenamyre JT, Cannon JR. 2015. Behavioral, neurochemical, and pathologic alterations in bacterial artificial chromosome transgenic G2019S leucine-rich repeated kinase 2 rats. *Neurobiology of aging* 36: 505-18
- Lee VM, Trojanowski JQ. 2006. Mechanisms of Parkinson's disease linked to pathological alpha-synuclein: new targets for drug discovery. *Neuron* 52: 33-8
- Lee Y, Dawson VL, Dawson TM. 2012. Animal models of Parkinson's disease: vertebrate genetics. *Cold Spring Harbor perspectives in medicine* 2
- Lesage S, Anheim M, Letournel F, Bousset L, Honore A, et al. 2013. G51D alpha-synuclein mutation causes a novel parkinsonian-pyramidal syndrome. *Annals of neurology* 73: 459-71
- Lesnick TG, Papapetropoulos S, Mash DC, Ffrench-Mullen J, Shehadeh L, et al. 2007. A genomic pathway approach to a complex disease: axon guidance and Parkinson disease. *PLoS genetics* 3: e98
- Li JY, Englund E, Holton JL, Soulet D, Hagell P, et al. 2008. Lewy bodies in grafted neurons in subjects with Parkinson's disease suggest host-to-graft disease propagation. *Nature medicine* 14: 501-3
- Liang WS, Reiman EM, Valla J, Dunckley T, Beach TG, et al. 2008. Alzheimer's disease is associated with reduced expression of energy metabolism genes in posterior cingulate neurons. *Proceedings of the National Academy of Sciences of the United States of America* 105: 4441-6

- Lill CM. 2016. Genetics of Parkinson's disease. *Molecular and cellular probes* 30: 386-96
- Lin CW, Hsueh YP. 2014. Sarm1, a neuronal inflammatory regulator, controls social interaction, associative memory and cognitive flexibility in mice. *Brain, behavior, and immunity* 37: 142-51
- Lin MT, Beal MF. 2006. Mitochondrial dysfunction and oxidative stress in neurodegenerative diseases. *Nature* 443: 787-95
- Liu HY, Chen CY, Hsueh YP. 2014. Innate immune responses regulate morphogenesis and degeneration: roles of Toll-like receptors and Sarm1 in neurons. *Neuroscience bulletin* 30: 645-54
- Liu Z, Zhou T, Ziegler AC, Dimitrion P, Zuo L. 2017. Oxidative Stress in Neurodegenerative Diseases: From Molecular Mechanisms to Clinical Applications. 2017: 2525967
- Lockhart PJ, Lincoln S, Hulihan M, Kachergus J, Wilkes K, et al. 2004. DJ-1 mutations are a rare cause of recessively inherited early onset parkinsonism mediated by loss of protein function. *Journal of medical genetics* 41: e22
- Loreto A, Di Stefano M, Gering M, Conforti L. 2015. Wallerian Degeneration Is Executed by an NMN-SARM1-Dependent Late Ca(2+) Influx but Only Modestly Influenced by Mitochondria. *Cell reports* 13: 2539-52
- Love S. 1999. Oxidative stress in brain ischemia. *Brain pathology (Zurich, Switzerland)* 9: 119-31
- Lubomski M, Louise Rushworth R, Lee W, Bertram KL, Williams DR. 2014. Sex differences in Parkinson's disease. *Journal of clinical neuroscience : official journal of the Neurosurgical Society of Australasia* 21: 1503-6
- Lucking CB, Brice A. 2000. Alpha-synuclein and Parkinson's disease. *Cellular and molecular life sciences : CMLS* 57: 1894-908
- Maesawa S, Kaneoke Y, Kajita Y, Usui N, Misawa N, et al. 2004. Long-term stimulation of the subthalamic nucleus in hemiparkinsonian rats: neuroprotection of dopaminergic neurons. *Journal of neurosurgery* 100: 679-87
- Malkus KA, Tsika E, Ischiropoulos H. 2009. Oxidative modifications, mitochondrial dysfunction, and impaired protein degradation in Parkinson's disease: how neurons are lost in the Bermuda triangle. *Molecular neurodegeneration* 4: 24
- Marongiu R, Ferraris A, Ialongo T, Michiorri S, Soleti F, et al. 2008. PINK1 heterozygous rare variants: prevalence, significance and phenotypic spectrum. *Human mutation* 29: 565
- Melrose HL, Lincoln SJ, Tyndall GM, Farrer MJ. 2006. Parkinson's disease: a rethink of rodent models. *Experimental brain research* 173: 196-204
- Meng F, Wang J, Ding F, Xie Y, Zhang Y, Zhu J. 2017. Neuroprotective effect of matrine on MPTP-induced Parkinson's disease and on Nrf2 expression. *Oncology letters* 13: 296-300
- Meredith GE, Kang UJ. 2006. Behavioral models of Parkinson's disease in rodents: a new look at an old problem. *Movement disorders : official journal of the Movement Disorder Society* 21: 1595-606
- Milde S, Gilley J, Coleman MP. 2013. Subcellular localization determines the stability and axon protective capacity of axon survival factor Nmnat2. *PLoS biology* 11: e1001539
- Moussaud S, Jones DR, Moussaud-Lamodiere EL, Delenclos M, Ross OA, McLean PJ. 2014. Alpha-synuclein and tau: teammates in neurodegeneration? *Molecular neurodegeneration* 9: 43
- Murata H, Sakaguchi M, Kataoka K, Huh NH. 2013. SARM1 and TRAF6 bind to and stabilize PINK1 on depolarized mitochondria. *Molecular biology of the cell* 24: 2772-84
- Musacchio T, Rebenstorff M, Fluri F, Brotchie JM, Volkman J, et al. 2017. Subthalamic nucleus deep brain stimulation is neuroprotective in the A53T alpha-synuclein Parkinson's disease rat model. *Annals of neurology* 81: 825-36

- Nalls MA, Pankratz N, Lill CM, Do CB, Hernandez DG, et al. 2014. Large-scale meta-analysis of genome-wide association data identifies six new risk loci for Parkinson's disease. *Nature genetics* 46: 989-93
- Nalls MA, Plagnol V, Hernandez DG, Sharma M, Sheerin UM, et al. 2011. Imputation of sequence variants for identification of genetic risks for Parkinson's disease: a meta-analysis of genome-wide association studies. *Lancet (London, England)* 377: 641-9
- Neumann M, Muller V, Kretschmar HA, Haass C, Kahle PJ. 2004. Regional distribution of proteinase K-resistant alpha-synuclein correlates with Lewy body disease stage. *Journal of neuropathology and experimental neurology* 63: 1225-35
- Nuber S, Harmuth F, Kohl Z, Adame A, Trejo M, et al. 2013. A progressive dopaminergic phenotype associated with neurotoxic conversion of alpha-synuclein in BAC-transgenic rats. *Brain : a journal of neurology* 136: 412-32
- Olanow CW, Mcnaught KS. 2006. Ubiquitin-proteasome system and Parkinson's disease. *Movement Disorders* 21: 1806-23
- Osterloh JM, Yang J, Rooney TM, Fox AN, Adalbert R, et al. 2012. dSarm/Sarm1 is required for activation of an injury-induced axon death pathway. *Science (New York, N.Y.)* 337: 481-4
- Ottolini D, Cali T, Negro A, Brini M. 2013. The Parkinson disease-related protein DJ-1 counteracts mitochondrial impairment induced by the tumour suppressor protein p53 by enhancing endoplasmic reticulum-mitochondria tethering. *Human molecular genetics* 22: 2152-68
- Paisánruíz C, Jain S, Evans EW, Gilks WP, Simón J, et al. 2004. Cloning of the gene containing mutations that cause PARK8-linked Parkinson's disease. *Neuron* 44: 595-600
- Pan-Montojo F, Anichtchik O, Dening Y, Knels L, Pursche S, et al. 2010. Progression of Parkinson's disease pathology is reproduced by intragastric administration of rotenone in mice. *PLoS one* 5: e8762
- Park J, Kim SY, Cha GH, Lee SB, Kim S, Chung J. 2005. Drosophila DJ-1 mutants show oxidative stress-sensitive locomotive dysfunction. *Gene* 361: 133-9
- Park J, Lee SB, Lee S, Kim Y, Song S, et al. 2006. Mitochondrial dysfunction in Drosophila PINK1 mutants is complemented by parkin. *Nature* 441: 1157-61
- Peters CM, Gartner CE, Silburn PA, Mellick GD. 2006. Prevalence of Parkinson's disease in metropolitan and rural Queensland: a general practice survey. *Journal of clinical neuroscience : official journal of the Neurosurgical Society of Australasia* 13: 343-8
- Pezzoli G, Cereda E. 2013. Exposure to pesticides or solvents and risk of Parkinson disease. *Neurology* 80: 2035-41
- Plunfavreau H, Klupsch K, Moiso N, Gandhi S, Kjaer S, et al. 2007. The mitochondrial protease HtrA2 is regulated by Parkinson's disease-associated kinase PINK1. *Nature Cell Biology* 9: 1243-52
- Polymeropoulos MH, Higgins JJ, Golbe LI, Johnson WG, Ide SE, et al. 1996. Mapping of a gene for Parkinson's disease to chromosome 4q21-q23. *Science (New York, N.Y.)* 274: 1197-9
- Polymeropoulos MH, Lavedan C, Leroy E, Ide SE, Dehejia A, et al. 1997. Mutation in the alpha-synuclein gene identified in families with Parkinson's disease. *Science (New York, N.Y.)* 276: 2045-7
- Pringsheim T, Jette N, Frolkis A, Steeves TD. 2014. The prevalence of Parkinson's disease: a systematic review and meta-analysis. *Movement disorders : official journal of the Movement Disorder Society* 29: 1583-90
- Przedborski S, Jackson-Lewis V, Naini AB, Jakowec M, Petzinger G, et al. 2001. The parkinsonian toxin 1-methyl-4-phenyl-1,2,3,6-tetrahydropyridine (MPTP): a technical review of its utility and safety. *Journal of neurochemistry* 76: 1265-74

- Przedborski S, Levivier M, Jiang H, Ferreira M, Jackson-Lewis V, et al. 1995. Dose-dependent lesions of the dopaminergic nigrostriatal pathway induced by intrastriatal injection of 6-hydroxydopamine. *Neuroscience* 67: 631-47
- Ramsey CP, Glass CA, Montgomery MB, Lindl KA, Ritson GP, et al. 2007. Expression of Nrf2 in neurodegenerative diseases. *Journal of neuropathology and experimental neurology* 66: 75-85
- Rhinn H, Qiang L, Yamashita T, Rhee D, Zolin A, et al. 2012. Alternative alpha-synuclein transcript usage as a convergent mechanism in Parkinson's disease pathology. *Nature communications* 3: 1084
- Riederer BM, Draberova E, Viklicky V, Draber P. 1995. Changes of MAP2 phosphorylation during brain development. *The journal of histochemistry and cytochemistry : official journal of the Histochemistry Society* 43: 1269-84
- Schapira AH. 1994. Evidence for mitochondrial dysfunction in Parkinson's disease--a critical appraisal. *Movement disorders : official journal of the Movement Disorder Society* 9: 125-38
- Schober A. 2004. Classic toxin-induced animal models of Parkinson's disease: 6-OHDA and MPTP. *Cell and tissue research* 318: 215-24
- Seto E, Yoshida M. 2014. Erasers of histone acetylation: the histone deacetylase enzymes. *Cold Spring Harbor perspectives in biology* 6: a018713
- Shaikh KT, Yang A, Youshin E, Schmid S. 2015. Transgenic LRRK2 (R1441G) rats-a model for Parkinson disease? *PeerJ* 3: e945
- Sharma S, Taliyan R. 2015. Targeting histone deacetylases: a novel approach in Parkinson's disease. *Parkinson's disease* 2015: 303294
- Shaw-Smith C, Pittman AM, Willatt L, Martin H, Rickman L, et al. 2006. Microdeletion encompassing MAPT at chromosome 17q21.3 is associated with developmental delay and learning disability. *Nature genetics* 38: 1032-7
- Sherer TB, Kim JH, Betarbet R, Greenamyre JT. 2003. Subcutaneous rotenone exposure causes highly selective dopaminergic degeneration and alpha-synuclein aggregation. *Experimental neurology* 179: 9-16
- Shin RW, Iwaki T, Kitamoto T, Tateishi J. 1991. Hydrated autoclave pretreatment enhances tau immunoreactivity in formalin-fixed normal and Alzheimer's disease brain tissues. *Laboratory investigation; a journal of technical methods and pathology* 64: 693-702
- Siddiqui IJ, Pervaiz N, Abbasi AA. 2016. The Parkinson Disease gene SNCA: Evolutionary and structural insights with pathological implication. *Scientific reports* 6: 24475
- Singleton AB, Farrer M, Johnson J, Singleton A, Hague S, et al. 2003. alpha-Synuclein locus triplication causes Parkinson's disease. *Science (New York, N.Y.)* 302: 841
- Sloan M, Alegre-Abarrategui J, Potgieter D, Kaufmann AK, Exley R, et al. 2016. LRRK2 BAC transgenic rats develop progressive, L-DOPA-responsive motor impairment, and deficits in dopamine circuit function. *Human molecular genetics* 25: 951-63
- Smith WW, Jiang H, Pei Z, Tanaka Y, Morita H, et al. 2005. Endoplasmic reticulum stress and mitochondrial cell death pathways mediate A53T mutant alpha-synuclein-induced toxicity. *Human molecular genetics* 14: 3801-11
- Soldner F, Stelzer Y, Shivalila CS, Abraham BJ, Latourelle JC, et al. 2016. Parkinson-associated risk variant in distal enhancer of alpha-synuclein modulates target gene expression. *Nature* 533: 95-9
- Spieles-Engemann AL, Behbehani MM, Collier TJ, Wohlgenant SL, Steece-Collier K, et al. 2010. Stimulation of the rat subthalamic nucleus is neuroprotective following significant nigral dopamine neuron loss. *Neurobiology of disease* 39: 105-15
- Spillantini MG, Schmidt ML, Lee VM, Trojanowski JQ, Jakes R, Goedert M. 1997. Alpha-synuclein in Lewy bodies. *Nature* 388: 839-40

- Stauch KL, Villeneuve LM, Purnell PR, Pandey S, Guda C, Fox HS. 2016. SWATH-MS proteome profiling data comparison of DJ-1, Parkin, and PINK1 knockout rat striatal mitochondria. *Data in brief* 9: 589-93
- Su RJ, Zhen JL, Wang W, Zhang JL, Zheng Y, Wang XM. 2018. Time-course behavioral features are correlated with Parkinson's disease-associated pathology in a 6-hydroxydopamine hemiparkinsonian rat model. *Molecular medicine reports* 17: 3356-63
- Sun J, Kouranova E, Cui X, Mach RH, Xu J. 2013. Regulation of dopamine presynaptic markers and receptors in the striatum of DJ-1 and Pink1 knockout rats. *Neuroscience letters* 557 Pt B: 123-8
- Tang Y, Zhao W, Chen Y, Zhao Y, Gu W. 2008. Acetylation is indispensable for p53 activation. *Cell* 133: 612-26
- Tipton KF, Singer TP. 1993. Advances in our understanding of the mechanisms of the neurotoxicity of MPTP and related compounds. *Journal of neurochemistry* 61: 1191-206
- Van Den Eeden SK, Tanner CM, Bernstein AL, Fross RD, Leimpeter A, et al. 2003. Incidence of Parkinson's disease: variation by age, gender, and race/ethnicity. *American journal of epidemiology* 157: 1015-22
- Van der Perren A, Toelen J, Casteels C, Macchi F, Van Rompuy AS, et al. 2015. Longitudinal follow-up and characterization of a robust rat model for Parkinson's disease based on overexpression of alpha-synuclein with adeno-associated viral vectors. *Neurobiology of aging* 36: 1543-58
- Villeneuve LM, Purnell PR, Boska MD, Fox HS. 2016. Early Expression of Parkinson's Disease-Related Mitochondrial Abnormalities in PINK1 Knockout Rats. *Molecular neurobiology* 53: 171-86
- von Bohlen Und Halbach O. 2005. Modeling neurodegenerative diseases in vivo review. *Neurodegenerative diseases* 2: 313-20
- Walker MD, Volta M, Cataldi S, Dinelle K, Beccano-Kelly D, et al. 2014. Behavioral deficits and striatal DA signaling in LRRK2 p.G2019S transgenic rats: a multimodal investigation including PET neuroimaging. *Journal of Parkinson's disease* 4: 483-98
- Wang H, Dharmalingam P, Vasquez V, Mitra J, Boldogh I, et al. 2017. Chronic oxidative damage together with genome repair deficiency in the neurons is a double whammy for neurodegeneration: Is damage response signaling a potential therapeutic target? *Mechanisms of ageing and development* 161: 163-76
- Williams DR, Hadeed A, al-Din AS, Wreikat AL, Lees AJ. 2005. Kufor Rakeb disease: autosomal recessive, levodopa-responsive parkinsonism with pyramidal degeneration, supranuclear gaze palsy, and dementia. *Movement disorders : official journal of the Movement Disorder Society* 20: 1264-71
- Wills J, Jones J, Haggerty T, Duka V, Joyce JN, Sidhu A. 2010. Elevated tauopathy and alpha-synuclein pathology in postmortem Parkinson's disease brains with and without dementia. *Experimental neurology* 225: 210-8
- Wood-Kaczmar A, Gandhi S, Wood NW. 2006. Understanding the molecular causes of Parkinson's disease. *Trends in molecular medicine* 12: 521-8
- Wright Willis A, Evanoff BA, Lian M, Criswell SR, Racette BA. 2010. Geographic and ethnic variation in Parkinson disease: a population-based study of US Medicare beneficiaries. *Neuroepidemiology* 34: 143-51
- Xiong X, Hao Y, Sun K, Li J, Li X, et al. 2012. The Highwire ubiquitin ligase promotes axonal degeneration by tuning levels of Nmnat protein. *PLoS biology* 10: e1001440
- Yamada M, Mizuno Y, Mochizuki H. 2005. Parkin gene therapy for alpha-synucleinopathy: a rat model of Parkinson's disease. *Human gene therapy* 16: 262-70
- Yang Y, Gehrke S, Haque ME, Imai Y, Kosek J, et al. 2005. Inactivation of Drosophila DJ-1 leads to impairments of oxidative stress response and phosphatidylinositol 3-kinase/Akt

- signaling. *Proceedings of the National Academy of Sciences of the United States of America* 102: 13670-5
- Yokota T, Sugawara K, Ito K, Takahashi R, Ariga H, Mizusawa H. 2003. Down regulation of DJ-1 enhances cell death by oxidative stress, ER stress, and proteasome inhibition. *Biochemical and biophysical research communications* 312: 1342-8
- Zarranz JJ, Alegre J, Gomez-Esteban JC, Lezcano E, Ros R, et al. 2004. The new mutation, E46K, of alpha-synuclein causes Parkinson and Lewy body dementia. *Annals of neurology* 55: 164-73
- Zhang X, Gao F, Wang D, Li C, Fu Y, et al. 2018. Tau Pathology in Parkinson's Disease. *Frontiers in neurology* 9: 809

7 List of figures and tables

Figure 1: Schematic illustration of the direct and indirect pathway in under physiological conditions and in PD.....	10
Figure 2: Schematic image of multiple pathogenesis of PD.....	12
Figure 3: Images showing rat movements in behavioral tests.....	25
Figure 4: Stereotaxic injection in rat brain.....	26
Figure 5: Immunohistochemical staining for TH as marker of the dopaminergic tract..	32
Figure 6: Immunofluorescence double stainings of human aSyn (green) and TH (red)..	34
Figure 7: Results of behavioral tests of EV and A53T-aSyn rat groups respectively 2 weeks, 4 weeks and 6 weeks after injection.....	35
Figure 8: Relative optical density or relative cell number in the TH+ dopaminergic tract of EV and A53T-aSyn rat groups respectively 2 weeks, 4 weeks and 6 weeks after injection.....	36
Figure 9: TH stainings and estimated cell number of TH+ SN neurons in pre-op, EV and A53T-aSyn rat groups respectively 2 weeks, 4 weeks and 6 weeks after injection.....	38
Figure 10: Motor deficits in haSyn PD rats correlate with dopaminergic terminal loss in the striatum.....	39
Figure 11: Immunofluorescence stainings and intensity analysis of Nrf2 expression in the dopaminergic nigrostriatal tract of EV and A53T-aSyn rat groups respectively 2 weeks, 4 weeks and 6 weeks after injection.....	40
Figure 12: Immunofluorescence stainings and intensity analysis of Tau expression in the dopaminergic nigrostriatal tract of EV and A53T-aSyn rat groups respectively 2 weeks, 4 weeks and 6 weeks after injection.....	42
Figure 13: Immunofluorescence stainings and intensity analysis of SARM1 expression in the dopaminergic nigrostriatal tract of EV and A53T-aSyn rat groups respectively 2 weeks, 4 weeks and 6 weeks after injection.....	45
Figure 14: Immunofluorescence stainings and intensity analysis of NMNAT2 expression in the dopaminergic nigrostriatal tract of EV and A53T-aSyn rat groups respectively 2 weeks, 4 weeks and 6 weeks after injection.....	46
Table 1: Alterations of pro- and antidegeneration markers (Nrf2, Tau, SARM1 and NMNAT2) in the nigrostriatal tract in the AAV1/2-A53T-aSyn PD rat model.....	58

8 Abbreviations

PD	Parkinson's disease
DA	dopaminergic
SNpc	substantia nigra pars compacta
LBs	Lewy bodies
aSyn	alpha-synuclein
wt	Wild-type
SNPs	single nucleotide polymorphisms
PRKN	Parkin protein
ER	endoplasmic reticulum
6-OHDA	6-hydroxydopamine
BBB	blood-brain barrier
AAV	adeno-associated viral
KO	knock-out
BG	basal ganglia
STR	striatum
GP	globus pallidus
STN	subthalamic nucleus
GPI	internal globus pallidus
Gpe	external globus pallidus
SNpr	substantia nigra pars reticulata
SNpc	substantia nigra pars compacta
THA	thalamus
GABA	gamma-aminobutyric acid
AD	Alzheimer's disease
Nrf2	Nuclear Factor Erythroid 2-Related Factor 2
OS	Oxidative Stress
ROS	reactive oxygen species
ARE	antioxidant reaction elements
WB	western blot
EtOH	Ethanol
HATs	histone acetyltransferase

histone deacetylase, HDAC

MAP

EV

histone deacetylase

microtubule-associated proteins

AAV1/2-empty vector

9 Note of thanks

First of all, I would like to express my sincere gratitude to China Scholarship Council, for supporting me during my MD study in Germany.

Further, I would like to thank all the Professors in my Professor's committee, especially Professor Jens Volkmann, who offered me the opportunity to pursue my doctoral study in the neurologic department of Würzburg university, and helped me solve several problems during my study.

I would like to thank my supervisor- Professor Chi Wang Ip, for all the time and efforts that he put in my research work.

I am also thankful to Luisa- the very nice technician in our lab, who helped me finish a few technical work of my research project.

Also thanks to two post docs in our lab- Flora Vitale from Italy and Katarina Lazic from Salvia, who gave me some good suggestions in both work and life, they are not only colleagues but also my friends.

And many thanks to Ms. Mewis Margit in doctoral office of the medical faculty, for her great patience in communicating with me in German and explaining me the details of the procedures for applying for MD degree.

I can not forget to thank my friends here in Germany who have put up with my stress, and shared with me the good time in Germany.

And my biggest thanks to my family for all the support you have shown me through this three years of distance learning, for all the unconditional support in this very intense academic year.